



Review

Potassium sodium niobate (KNN) lead-free piezoceramics: A review of phase boundary engineering based on KNN materials

Hidayah Mohd Ali Piah¹, Mohd Warikh Abd Rashid^{1,*}, Umar Al-Amani Azlan² and Maziat Akmal Mohd Hatta³

¹ Faculty of Manufacturing Engineering, Universiti Teknikal Malaysia Melaka, Hang Tuah Jaya, 76100 Durian Tunggal, Melaka, Malaysia

² Faculty of Mechanical and Manufacturing Engineering Technology, Universiti Teknikal Malaysia Melaka, Hang Tuah Jaya, 76100 Durian Tunggal, Melaka, Malaysia

³ Faculty of Engineering, International Islamic University Malaysia, 53100 Jalan Gombak, Kuala Lumpur, Malaysia

* **Correspondence:** Email: warikh@utem.edu.my; Tel: +6-06-270-1311.

Abstract: Lead zirconia titanate (PZT) is the most often used piezoelectric material in various electronic applications like energy harvesters, ultrasonic capacitors and motors. It is true that PZT has a lot of significant drawbacks due to its 60% lead content, despite its outstanding ferroelectric, dielectric and piezoelectric properties which influenced by PZT's morphotropic phase boundary. The recently found potassium sodium niobate (KNN) is one of the most promising candidates for a new lead-free piezoelectric material. For the purpose of providing a resource and shedding light on the future, this paper provides a summary of the historical development of different phase boundaries in KNN materials and provides some guidance on how to achieve piezoelectric activity on par with PZT through a thorough examination and critical analysis of relevant articles by providing insight and perspective of KNN, which consists of detailed evaluation of the design, construction of phase boundaries and engineering for applications.

Keywords: KNN; piezoelectric; lead-free; phase boundaries; phase transition temperature

1. Introduction

Piezoelectric material lead zirconia titanate (PZT) is widely used in a variety of electronic devices, including energy harvesters, ultrasonic capacitors and motors, because of its excellent ferroelectric, dielectric and piezoelectric properties. Even if there are a wide variety of applications and their market size is growing, the quest for new applications continues in the industries that are related with it. In part, this is owing to the rapid advancement of alternative technologies, which puts the existing market at risk of being overtaken at any time. It is true that despite its impressive electrical properties, PZT has several severe disadvantages. It contains over 60% lead [1]. According to the Comprehensive Environmental Response, Compensation, and Liability Act of 1980, lead is one of the most toxic substances that might potentially cause damage to the neurological system as well as the development of spermatozoid. Lead is on the list of most dangerous compounds because of its cancer-causing properties.

This paper will give a rundown of some of the more recent applications of lead-based and lead-free piezoceramics, as well as look ahead to possible future uses for these materials. For example, a great deal of work has been done to discover new types of piezoelectric materials. Potassium sodium niobate (KNN) is one of the most promising prospects for a new lead-free piezoelectric material that has been discovered as a result of these efforts. As recently as 2004, when Saito et al. reported on the development of KNN-based piezoceramics, the aim seemed to be within reach [2]. KNbO_3 (KN) and NaNbO_3 perovskites were combined to generate KNN, a new perovskite material (NN). In the A site, potassium and sodium ions are present, while niobium ions are present in the B site. Curie temperature was 420 °C, dielectric constant was 700, remanent polarisation was 14 $\mu\text{C}/\text{cm}^2$, low coercive field was 140 kV/cm^2 and high piezoelectric constant was 1.6 volts/cm [1,3,4].

In comparison to PZT, the piezoelectric characteristics of pure KNN are considerably lacking. Notably, this current work shows an unwavering commitment to the KNN-based system, whereas multiple outstanding evaluations have compared alternative lead-free piezoceramic in comparison [5–9]. There have been hundreds of articles in the previous decades about the development of KNN ceramics, indicating undeniable interest in this system as the most promising possibility for commercially viable lead-free piezoceramics candidates. A great deal of research has been devoted to the creation of KNN-based piezoelectrics and exceptionally promising piezoelectric qualities have been reported [10–12]. Li and co-workers wrote and published a comprehensive study of KNN-based materials focusing on their fundamental properties, processing processes, property change and beneficial applications. A comprehensive evaluation of the design, construction of phase boundaries and improvement of piezoelectric characteristics in KNN-based materials was published by Wu and colleagues [13]. Phase barriers in KNN-based materials have been studied extensively by the authors and they gave viable ideas for increasing piezoelectric activity in KNN-based materials [14]. KNN utilising doped KNN to improve its physical and electrical performance is also being studied by the researchers [15]. There has been a recent pattern of progressive growth in the number of papers discussing materials based on alkali niobium. Among these articles, the building of phase boundaries has emerged as a key method for the enhancement of the electrical properties of these materials. As a consequence of this, phase boundaries play a crucial part in the overall development of alkali niobium lead-free piezoelectrics [13]. According to the findings in this paper, the current state of KNN-based ceramics has been thoroughly assessed by a thorough examination and a critical analysis of relevant articles. As a result, we would

be thrilled if this study might serve as a useful resource and shed light on the future development of KNN-based materials.

2. Phase boundaries

In a macroscopically nonpolar ceramic, the employment of ferroelectric materials enables one to generate a unique polar axis by a so-called poling process, as explained by Jaffe et al. (1958). Inducing a piezoelectric effect in this ferroelectric material was revealed to be far more powerful than in previously studied single crystal piezoelectrics. Consequently, the success of developing the first polycrystalline piezoelectrics prompted a thorough search for improved piezoceramics, which ultimately resulted in the development of PZT ceramic solid solutions in the 1950s. During the poling process, it is generally agreed upon that a high degree of alignments of ferroelectric dipoles can be driven by a large amount of thermodynamically equivalent states when the material is subjected to a driving electric field, which makes it simple to generate enhanced electrical properties [16–39]. In the field of piezoelectric materials, PZT's morphotropic phase boundary (MPB) construction is regarded a typical case where the crystal structure undergoes a sudden transition and the piezoelectricity of the mixture is optimised at MPB [17,22,33,40].

The discovery of MPB-induced property enhancement has set a new standard for the future discovery of piezoceramics. The results of these studies have been published in a number of academic references. The change of phase boundaries is a potent instrument for the promotion of electrical properties of piezoelectric materials, the involved phase boundaries and their corresponding types are substantially responsible for the augmentation in piezoelectric activity, regardless of whether a material is lead based or lead free [10,15–17,27,28,32–72] is because the involved phase boundaries and their corresponding types.

There are three different types of phase transitions known to exist in KNN materials, corresponding to the temperatures at which the material changes from rhombohedral to orthorhombic (T_{R-O}), orthorhombic to tetragonal (T_{O-T}) and rhombohedral to tetragonal (T_{R-T}), respectively [6,73]. The temperature dependency of the individual dielectric peaks provides a clear illustration of T_{R-O} , T_{O-T} and T_C . The R-O or O-T phase boundary in KNN may be created at room temperature if the T_{R-O} or T_{O-T} temperature was shifted to room temperature by the use of additives. On the other hand, the phase boundary that corresponds to R-O or O-T possesses the polymorphic phase transition (PPT) characteristic [74–77] and it is dependent not only on the compositions but also on the temperatures, as shown in Figure 1. This is the case when R-O or O-T corresponds to a transition between two different types of phases. When the compositions of a piezomaterial are located at the phase boundaries, the polarisation of the material can be rotated more easily between different symmetries, which can result in an improvement in the material's dielectric and piezoelectric properties. This is true regardless of whether the material possesses MPB or PPT characteristics.

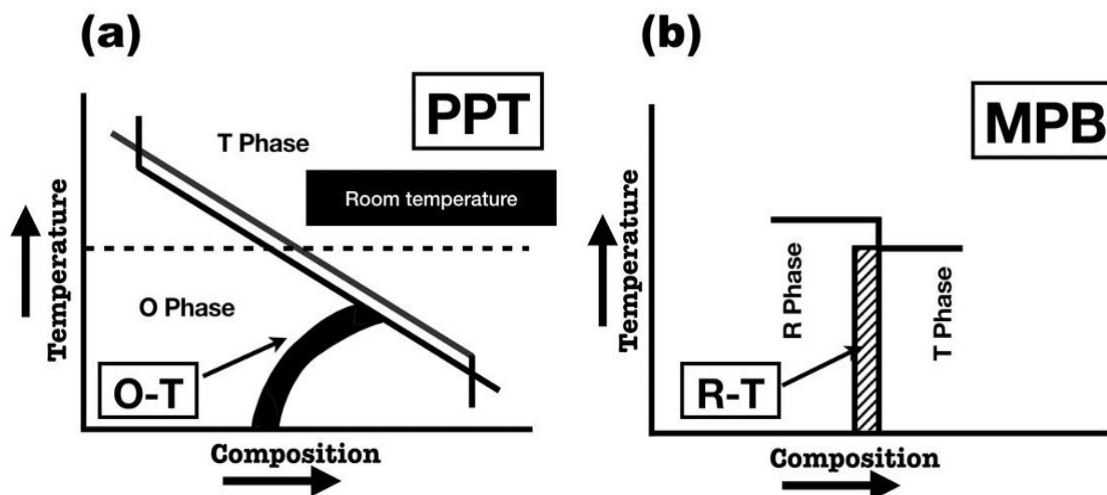


Figure 1. (a) Polymorphic phase transition (b) morphotropic phase boundary [13].

However, recent developments suggest that there is only a small improvement in the d_{33} values for KNN materials having O-T or R-O phase boundaries [12,37,38,76–78], which is inferior to the vast majority of PZT ceramics [3] or even textured KNN [10]. Since polarisation axis rotations are easily produced in compositions close to an R-T boundary, such boundaries may be required to further boost the piezoelectric activity of KNN [79,80]. This assumption has also been recently confirmed in potassium-sodium niobate piezoceramics by experimental methods [81–86] and a greater d_{33} value has been reached by creating R-T phase boundaries. In order to form R-T phase barrier, two or more additives such as Ta and Sb and few other additives must be used to simultaneously lower their T_{R-O} and raise their T_{O-T} values toward room temperature [71,87–89]. New concepts can thus be applied to the development of high-performance KNN-based materials.

A material's phase boundaries can be influenced by its chemical composition or other parameters [90–94] that define its electrical properties. Materials with compositions around the phase boundaries (e.g., R-O, R-T, or O-T) include $\text{Bi}_{0.5}\text{Na}_{0.5}\text{TiO}_3$, and $(\text{K},\text{Na})\text{NbO}_3$. Higher d_{33} values are often achievable with BaTiO_3 -based materials, but their low T_C makes them unsuitable for use in high-temperature environments. However, these materials can be used to make actuators that can function at temperatures below 100 °C. The low “depoling temperature” of $\text{Bi}_{0.5}\text{Na}_{0.5}\text{TiO}_3$ -based materials, like that of BaTiO_3 -based materials, limits their practical applications [95–99]. However, Jo et al. (2011), have created a huge strain that is equivalent or even superior to PZT. Figure 2a,b shows that the phase boundary types and the composition itself determine the width of the d_{33} and T_C distributions in KNN-based materials (e.g., $d_{33} = 171\text{--}490$ pC/N, $T_C = 178\text{--}475$ °C) [96]. In particular, by creating new R-T phase barriers, we were able to make significant progress in the piezoelectricity of KNN-based ceramics. The gap between lead-free and lead-based materials has been narrowed thanks to the development of novel phase boundaries that can be used to improve the piezoelectricity of KNN materials with all information taken directly from the sources cited. As can be seen in Figure 2a, PNN-based and relaxor PT single crystals with an MPB [93–94] exhibit a massive d_{33} value, whereas PZT-based materials exhibit a broad d_{33} distribution that is sensitive to the doping components. Recent research on PNN-based single crystal relaxors has shown a piezoelectric coefficient of 3500 pC/N [100]. Doping a relaxor ferroelectric crystal with rare-earth elements allowed for the measurement of this

value. This study is the latest one on the subject, having been completed in 2022. On the other hand, it is likely that fresh research has been carried out since then, which might provide information that is more up to date about the piezoelectric coefficient for PNN-based single crystal relaxor.

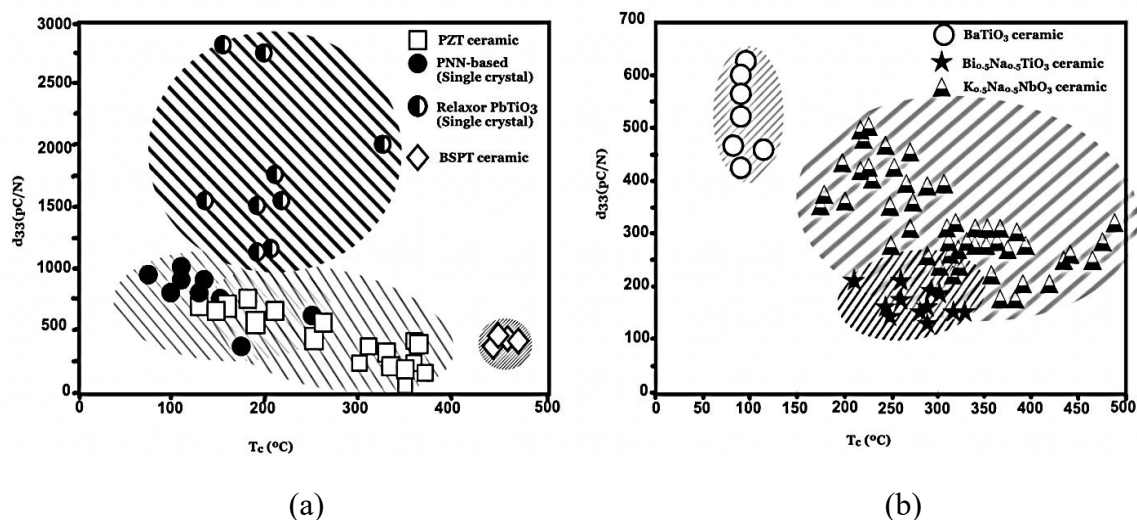


Figure 2. Value of d_{33} vs T_c of (a) lead-based (b) lead-free ceramics from number of researches [13].

2.1. Phase boundary identification

The phase boundary of KNN is the composition and temperature transition between distinct crystal structures. It is essential to have an understanding of the phase boundary in order to modify the properties of KNN-based materials to accommodate a variety of applications. Structure analysis methods including X-ray diffraction (XRD) and neutron diffraction are commonly used to determine where the phase boundary lies in KNN. Diffraction patterns can reveal the crystal structure of a material, allowing for the determination of its various phases. For instance, XRD was used in a study to determine the crystal structure and phase transitions of KNN perovskites [101]. For instance, the crystal structure of A-site substituted perovskite KNN compounds was determined using high-resolution XRD and neutron diffraction. Finding a phase-coexistence zone at the monoclinic-tetragonal phase transition provides evidence of a first-order phase barrier, as reported in previous research [102]. Researchers showed that XRD measurements may be used to distinguish between the various phases of KNN perovskites and to identify the region of transition between them T_{O-T} and T_{T-C} were detected at 236 and 440 °C, indicating a trend towards lower temperature side for phase transition temperatures [103].

However, identifying the temperature and composition regions where the phase transition occurs is essential for characterising the phase boundary. This data is essential for figuring out how KNN-based materials react in various environments. The phase boundary of KNN has been the subject of several studies that have utilised a variety of methods to characterise it. Examining KNN-based ceramic's piezoelectric and strain characteristics at varying compositions and temperatures is one of the methods. Zheng et al. (2015) looked at the conflicts between high strain and high piezoelectricity in KNN materials and proposed the creation of new phase boundaries to resolve the conflicts [104]. Using temperature-dependent XRD patterns, a study describes the structural evolution of the rhombohedral-

tetragonal (R-T) phase boundary in KNN-based ceramics. Rhombohedral, rhombohedral-orthorhombic and rhombohedral-tetragonal phases were all identified in the study [105]. Adding dopants or substitute components to KNN is another way to shift the phase boundary. KNN's orthorhombic-rhombohedral phase transition temperature was shown to be controllable via dopant concentration when barium zirconate was included into the material. This research showed that the compositional adjustments can be used to manipulate the phase boundary of KNN. In order to fully appreciate its characteristics and modify its behaviour for specific applications, it is crucial to locate and characterise the phase boundary of KNN. Crystal structure and symmetry of KNN at various compositions and temperatures are typically determined by structural analysis methods including XRD and neutron diffraction. The phase boundary can be characterised by analysing the effects of dopants or substitute elements on the phase transition and taking measurements of the piezoelectric and strain properties of KNN-based ceramics. These investigations aid in the creation of high-quality KNN-based materials.

3. Development of phase boundaries

In KNN-based piezoceramics, the polymorphic phase boundary (PPB) has been the primary focus of research, but there have been some attempts to actualize the MPB, or rhombohedral vs. tetragonal phase boundary, found in PZT. The primary motivation for doing so is to realise the lowest temperature rhombohedral phase in KNN under ambient conditions. KNN is an isotropic solid solution between the orthorhombic symmetry ferroelectric KN and the antiferroelectric NN [13,106,107]. KNN is quite different from PZT in that its phase diagram is extremely intricate, with three vertical MPBs between two distinct ferroelectric orthorhombic phases [108]. The one with a K content below 50% is particularly relevant. KNN has a high Curie temperature (420 °C), however its piezoelectric characteristics are subpar while it is at ambient temperature. Hot-pressed dense samples have been measured to have a maximum d_{33} of 160 pC/N and a k_2 of 0.3 [43]. As a result, the majority of previous research has concentrated on improving these functional qualities through chemical modifications. In this regard, BaZrO₃ was shown to be effective by Wang et al. [109]. There has been further research in this area as a result of this, leading to the empirical conclusion that Zr₄ appears to play a significant role [12,110]. These studies confirmed that KNN-based materials are capable of being fabricated into MPB similar to PZT. However, the induced MPB is likely to be skewed in the phase diagram of temperature versus composition. This MPB contradicts the group subgroup relationship since it is more akin to the PPB between rhombohedral and tetragonal. To improve the formulation of truly PZT-like MPB in KNN, that is, a vertical MPB between rhombohedral and tetragonal, further studies have been conducted on the idea that increasing the rhombohedral field in the PZT-like MPB compositions would make the existing rhombohedral symmetry more thermally-stable [110]. Since MPB existing at room temperature endures up to 250 °C with fairly strong functional qualities, it suggests that the notion is working despite its apparent simplicity. However, testing of this MPB's range needs to be done at temperatures at least 40 °C below room temperature. Here, we primarily examine how various phase boundaries in KNN materials have evolved over time and offer some guidance on how to achieve piezoelectric activity on par with PZT. Additionally, this article summarises the extensive discussions on how to build phase boundaries by chemical modifications.

3.1. Formation orthorhombic-tetragonal phase boundaries

Since a significant advancement in KNN-based materials, the O-T phase boundary has become the most well-known. One of the most contentious aims of research into KNN based materials is the establishment of the O-T phase border [111–113]. The original breakthrough in its d_{33} value occurred in 2004 when O-T phase coexistence was brought down to or near room temperature through the use of additives. In KNN-based textured ceramics, for instance, the coexistence of O and T phases at room temperature and the use of a new preparation technique led to a high d_{33} value of 416 pC/N, while LiNbO₃ or LiTaO₃-modified KNN ceramics achieved enhanced piezoelectric activity by constructing the same phase boundary using conventional solid-state methods. These pioneering works have stimulated a surge in interest in lead-free piezoelectrics around the world and as a result, scientists have focused considerable effort on fostering piezoelectric activity by erecting O-T phase boundaries. Several previous attempts to construct O-T phase boundaries in KNN-based ceramics in order to induce enhancement of its piezoelectric activity have met with success. These include ion substitutions, solid solutions with other ABO₃-type perovskites [98,99] or ABO₃ multicomponents [114–117].

3.1.1. Perovskite ABO₃ as a modifier

Perovskite ABO₃ materials, such as Bi_{0.5}A_{0.5}TiO₃ (A = Na⁺ [118,119], K⁺ [120], Li⁺ [121]), BTiO₃ (B = Ba²⁺, Sr²⁺ [122], Ca²⁺ [123], (Ba_{0.95}Sr_{0.05})²⁺ [124], [(Bi_{0.5}Na_{0.5})_{0.94}Ba_{0.06}]²⁺ [125] or BiMO₃ (M = Sc³⁺ [126], Al³⁺ [127], Fe³⁺ [114], Co³⁺ [115]) and others could lowering T_{O-T} values. ABO₃ doping can efficiently stimulate the establishment of O-T phase barriers resulting in increased of piezoelectricity [124]. Even while the addition of ABO₃-type additives can improve the d_{33} values of KNN-based materials [115], the resulting values are still lower than those of KNN ceramics including Li⁺, Ta⁵⁺ and Sb⁵⁺ [68,128,129]. However, ABO₃'s low price makes it a possible choice for real-world applications. KNN ceramics doped with ABO₃ multicomponents commonly possess improved piezoelectric activity ($d_{33} = 220\text{--}305$ pC/N) combined with high T_C values of >300 °C, as indicated in Table 1. The results reveal that O-T phase barriers can occur when the T_{O-T} transition temperature of a material is shifted to room temperature via doping with most ABO₃ multicomponents.

Table 1. Material system of KNN.

KNN material system	d_{33}	(pC/N) kp	T _c (°C)	Ref.
0.97(K _{0.5} Na _{0.5})NbO ₃ -0.03(Bi _{0.5} Na _{0.5})TiO ₃	195	0.43	375	[118]
(1-x)K _{0.5} Na _{0.5} NbO ₃ -0.06BiFeO ₃	146	0.51	405	[130]
K _{0.5} Na _{0.5} NbO ₃ -LiTaO ₃ -0.1MnO ₂	251	29.5	330–350	[131]
0.96(K _{0.5} Na _{0.5}) _{0.95} Li _{0.05} Nb _{0.93} Sb _{0.07} O ₃ -0.04CaZrO ₃	420	-	-	[132]
0.993(K,Na)NbO ₃ -0.007BiFeO ₃	220	0.46	-	[132]
(K _{0.5} Na _{0.5})NbO ₃ -0.01Bi(Ni _{2/3} Nb _{1/3})O ₃	150	-	300–400	[133]
(0.97-x)K _{0.40} Na _{0.60} Nb _{0.95} Sb _{0.05} O ₃ -0.03Bi _{0.5} K _{0.5} HfO ₃ -0.01SrZrO ₃	280	0.364	-	[134]

Doping with BiFeO₃ or BiScO₃ is particularly promising for enhancing d_{33} in BiMeO₃ (Me = Fe, Sc, Al, etc.) additives and d_{33} values of >250 pC/N are frequently produced in such ternary systems via the creation of O-T phase barriers [113,135]. Variations in the magnitude of the increase in d_{33} are largely attributable to the rates at which T-O and T are being shifted. For example, Jiang et al. studied KNN-LiSbO₃-BiFeO₃ ternary systems in order to shift the T_{O-T} close to room temperature, finding that low quantities of BiFeO₃ (0.4 mol%) enhance the d_{33} values from 202 to 260 pC/N [135]. This means that BiFeO₃, as an ABO₃ component, can effectively increase the piezoelectric activity of KNNLiSbO₃ ceramics by generating O-T phase barriers at or near room temperature. Pure tetragonal structures were obtained in the ternary system K_{0.5}Na_{0.5}NbO₃LiSbO₃BiScO₃, demonstrating a d_{33} value of 305 pC/N which the researchers reasoned that the phase boundary could not have played a significant role in the enhanced piezoelectric capabilities [136]. In contrast, we discovered that BiScO₃ addition increases T_{R-O} values and decreases T_{O-T} values of KNN [81,82], allowing for the formation of the new R-T phase boundary at ambient temperature. Furthermore, at room temperature or lower, the dielectric constant of this material gradually increases, which may indicate the presence of phase barriers. Therefore, more research into this material system is required to determine where the increased piezoelectricity comes from [136].

For Bi_{0.5}K_{0.5}Zr_{0.9}Hf_{0.103} (BKZH) doped KNN based piezoceramics, Li and co-workers analysed the effects of BKZH doping in 2017 [137]. As the BKZH concentration increased, they found that the T_{O-T} decreased and the T_{R-O} increased. Therefore, BKZH doping aids in achieving room-temperature coexistence of various phases. This aids in increasing the piezoelectric coefficient (d_{33}), to the value of 451 pC/N. There are three different phases that can occur, such as rhombohedral, orthorhombic and tetragonal. They also discovered that adding 1 mol% BKZH lowered the T_C by 20 °C. Another work by Li et al. [138] looked at the impacts of ZrO₃ (BLKZ) as a dopant on (Bi_{0.45}La_{0.05}K_{0.5}) and observed comparable effects on phase transition temperatures. The incorporation of BLKZ resulted in the formation of a new phase boundary at room temperature between the rhombohedral, orthorhombic and tetragonal phases. However, the KNN-BLKZ phase structure is only tetragonal when BLKZ is equal to or more than 5 mol%. At $d_{33} = 385$ pC/N and T_C = 245 °C, KNN-0.035BLKZ performs best. BiNaZrAO₃ type dopants are used by scientists to lower T_{O-T} and raise T_{R-O}, but they also lower T_C. In 2020, Qiao et al. [139] employed BiNaZrHfO₃ and found that the orthorhombic phase boundary could be reached at T_C = 235 °C. Shi et al. [140] looked into BiSmNaZrO₃ (BSNZ) with the aim of achieving high piezo characteristics with an R-O-T phase structure. The group managed to get $d_{33} = 508$ pC/N and T_C = 268 °C. In addition, CaBiNaZrO₃ was utilised as a dopant by Pan et al. [141]. They discovered that the dopant does not lower the curie temperature in C_xBNZ when the Ca content is less than or equivalent to 0.4. Dopants such as Ba_{0.5}Ca_{0.5}Zr_{0.5}Hf_{0.5}O₃ (BCZH) [142] and Ba(Li_{0.4}W_{0.6})O₃ (BLW) [143] reduce T_{O-T} but also reduce T_C.

3.1.2. O-T phase engineering

Previous studies using XRD patterns discovered that the KNL-(N_{0.9-x}TS_x) ceramic system has both orthorhombic symmetry (O) and tetragonal symmetry (T). The tetragonal symmetry-related peaks become more prominent in high-Sb content samples. A larger concentration of Sb⁵⁺ creates a structural alteration that modifies the T/O content in the structure, while on the one hand, the substitutional addition of Sb⁵⁺ should lower the cell (owing to the smaller ionic radius) shifting the peaks towards higher angles. It has been shown by other researchers that small cations in B-sites allow for the

coexistence of different phases (from rhombohedral-tetragonal to orthorhombic-tetragonal) at room temperature, thereby lowering the T_{O-T} towards room temperature [144,145].

Meanwhile, field emission scanning electron microscopy (FESEM) images show that the average grain size drops from 1.9 μm at $x = 0.00$ to 1.3 μm at $x = 0.04$, as Sb addition increases. Moreover, a nonhomogeneous microstructure is observed for the lowest Sb concentration ($x = 0.02$). As a matter of fact, the poor additive distribution over the entire sample causes grains with antimony to exhibit a restriction in their normal grain growth, while grains without or with low antimony concentration display grain sizes similar to the pure sample. Finally, at the greatest antimony content ($x = 0.04$), the improved additive distribution throughout the entire sample results in a more uniform microstructure with a smaller average grain size. Several parameters, including grain size, final microstructure, dielectric permittivity and density values, may have contributed to the identical values recorded for samples with $x = 0.02$ and 0.04 [146].

Improving piezoelectric characteristics has been viewed as a functional benefit of stabilising an O-T coexistence phase boundary around room temperature. In this case, the KNL-($\text{N}_{0.9-x}\text{TS}_x$) ceramic's ferroelectric properties will shed light on the implications of the Sb^{5+} substitution. Previous studies established that as the Sb^{5+} dopant concentration increased, the orthorhombic and tetragonal phases stabilised close to R-T (making a threshold of multiphase coexistence where the tetragonal phase is predominant), leading to enhanced ferroelectric properties at $x = 0.02$. It is well established that various phases exhibit polarisation in distinct directions. Since there are six possible polarisation directions in the tetragonal phase and twelve in the orthorhombic phase, when their coexistence is stabilised, a total of 18 polarisation directions are viable. Ferroelectric behaviour due to spontaneous polarisation was consistently observed in all samples when tested in a strong external electric field [147].

Therefore, the study showed that the O-T phase coexistence phase boundary could be stabilised by substituting Sb ions in the perovskite structure, which also causes an increased degree of polarisation directions near room temperature, easing the polarisation process of the system, and where the average grain size also increases, encouraging the increased domain size and favouring more domain walls.

3.2. Formation of rhombohedral-orthorhombic phase boundaries

The Curie temperature of undoped KNN is more than 400 $^{\circ}\text{C}$ (T_C). Both the rhombohedral-to-orthorhombic (T_{R-O}) and the orthorhombic-to-tetragonal (T_{O-T}) transition temperatures are present (T_{O-T}). On the other hand, there are two major drawbacks of KNN-based lead-free ceramics. The piezoelectricity is low, only 80–180 pC/N [2,142,143,148–151]. Low sintered densification is another issue that makes manufacturing challenging since the R-O phase boundary of KNN occurs at relatively cold temperatures (about -123°C) [128,129] and yields a subpar d_{33} which is frequently disregarded. The T_{R-O} values of KNN have recently been boosted with the addition of additives such as Sb^{5+} [75,151,152], Ta^{5+} [153], AZrO_3 ($A = \text{Ba}^{2+}, \text{Sr}^{2+}, \text{Ca}^{2+}$) [138,139], BiScO_3 [154], etc. For example, the coexistence of R-O ferroelectric mixed phases has been shown to improve d_{33} (230 pC/N) and the T_{R-O} value of $(\text{K}_{0.48}\text{Na}_{0.52})(\text{Nb,Sb})\text{O}_3$ can be controlled to near room temperature by refining the Sb concentration [75]. In addition, it was discovered that doping with Ta^{5+} may reduce T_C and T_{O-T} while simultaneously increasing T_{R-O} of KNN [153], in a manner that was comparable to that of Sb^{5+} [75]. When AZrO_3 ($A = \text{Ba}^{2+}, \text{Sr}^{2+}, \text{or Ca}^{2+}$) is added to a pure KNN ceramic, the T_{R-O} temperature is lowered to room temperature [109]. The R-O phase boundary and the types of chemical modifications also

influence their d_{33} values, but increasing the d_{33} typically necessitates reducing the T_C [12,75,154]. It may be possible to build new phase boundaries (e.g., R-T) by simultaneously shifting T_{O-T} and T_{R-O} close to room temperature, despite the fact that R-O KNN materials have poor overall performance of d_{33} and T_C .

3.2.1. R-O phase engineering

In a particular research paper, CaZrO_3 was used as a modifier to develop $(\text{K}_{0.48}\text{Na}_{0.48}\text{Li}_{0.04})(\text{Nb}_{0.95}\text{Sb}_{0.05})\text{O}_3$ lead free ceramics. The CZ-KNLNS powders have a cubic structure and their particles average between 300 and 700 nm in size. It is clear that the addition of CaZrO_3 slows down particle growth because the particle size reduces when the amount of CaZrO_3 is increased. As the ceramic part becomes denser, the grain size decreases and the grain boundaries become undetectable. CaZrO_3 may have accumulated at the grain borders, inhibiting growth and causing the decrease in grain size. Research demonstrated that by adjusting the CaZrO_3 concentration, the phase constitution and domain structure of CZ-KNLNS ceramics may be modified. The presence of rhombohedral (R) phase characteristics at $x = 0.06$ indicates a steady decrease in the quantity of orthorhombic phase and an increase in the amount of R phase. This region is where the orthorhombic and rhombohedral (O-R) phases can coexist. Doping ions of different radii are introduced into the KNLNS ceramic lattice, with the smaller ion replacing the A site and the bigger ion replacing the B site. This leads to a smaller average ionic radius for the A-site and a larger average ionic radius for the B-site, leading the R phase to develop in the KNLNS at temperatures close to room temperature. Multi-phase coexistence is thought to play a significant role in the high quality of KNLNS based ceramics [155]. The findings showed the coexistence zone of orthorhombic-rhombohedral (O-R) phase can be thought of as occurring between $x = 0.03$ and $x = 0.06$, as the phase structure changed from orthorhombic to rhombohedral with increasing CaZrO_3 content. The ceramics exhibit a coexisting rhombohedral and orthorhombic phase structure at $x = 0.04$. The piezoelectricity of a material can be enhanced by applying a polarised electric field, as the electric domain of a multi-phase coexisting structure can be switched more easily than in a single-phase structure [155,156]. The enhanced piezoelectric characteristics are a result of the combination of a dense homogenous microstructure and a stable domain configuration at $x = 0.04$.

3.3. Formation of rhombohedral-tetragonal

Considering that the R-T phase boundary of PZT exhibits large d_{33} and a weak temperature dependency of piezoelectric capabilities [3], we wondered if a similar R-T phase boundary might be produced in KNN materials to further enhance their piezoelectric properties and temperature stability. Several studies suggest that it is possible to engineer a R-T phase boundary in KNN by controlling the establishment of R-O and O-T phase borders via doping in additives [12,32,75,154,157–162]. It is possible to raise T_{R-O} and decrease T_{O-T} of KNN materials by adding ions or ABO_3 materials (e.g., Sb^{5+} [75], Ta^{5+} [153], BaZrO_3 [160], CaZrO_3 [161], SrZrO_3 [161]). As a result, it is probable that the R-T phase barrier should be produced in KNN materials by changing the composition ratios of the doped additives. Doping with various additives in earlier investigations led to the eventual induction of the R-T phase boundary in KNN. Since then, a number of material systems based on KNN have been produced that have R-T phase borders [80,81,83,139,140]. By fabricating the R-T phase boundary

we found that the high d_{33} value in $0.96(\text{K}_{0.5}\text{Na}_{0.5})_{0.95}\text{Li}_{0.05}\text{Nb}_{1-x}\text{Sb}_x\text{O}_3-0.04\text{BaZrO}_3$ ceramics reported by researchers in 2013 (425 pC/N) matched the results reported for textured KNN-based ceramics (416 pC/N) [10,163–165]. In this work, Sb^{5+} and BaZrO_3 are employed together to improve the $T_{\text{R-O}}$ and reduce the $T_{\text{O-T}}$ of KNN materials [75,165]. Despite the huge d_{33} (344–425 pC/N), ceramics typically have T_{C} values of 200 °C [71,89,104]. This means that for efficient phase boundary design, both a larger T_{C} and a larger d_{33} in KNN are necessary [83,85,166].

Doping CZrO_3 ($\text{C} = \text{Ba}^{2+}, \text{Sr}^{2+}, \text{Ca}^{2+}$) has previously been reported to create three distinct phase transition temperatures (i.e., T_{C} , $T_{\text{R-O}}$, and $T_{\text{O-T}}$) in KNN [145]. Furthermore, Zr^{4+} plays a significant influence in the phase transition temperatures (particularly $T_{\text{R-O}}$). Ramajo et al. (2013) observed that adding Zr^{4+} softened the material's ferroelectric characteristics and improved its density, even though effects of CZrO_3 on T_{C} , $T_{\text{R-O}}$ and $T_{\text{O-T}}$ are mostly independent of A site type [82,104,151,165,167]. It has been reported before that KNN materials' $T_{\text{O-T}}$ can be changed by adding Bi^{3+} . Therefore, the R-T phase boundary can be formed by changing the $T_{\text{R-O}}$ and $T_{\text{O-T}}$ of KNN concurrently using additives containing two such elements, such as Bi^{3+} and Zr^{4+} . Furthermore, it is crucial to remember that the R-T phase boundary can be produced by employing the aforementioned chemicals, resulting in a significant d_{33} of 400–490 pC/N [92,145,146]. In comparison to other phase boundaries (such as O-T and R-O), the R-T phase boundary is a more effective technique to boost the piezoelectric activity of KNN based ceramics. Furthermore, d_{33} and T_{C} outperform BT and BNT-based materials across the board in KNN. Our discovery may lead the way for lead-free ceramics to be used in the real world, as the R-T phase barrier considerably enhances the piezoelectric activity of KNN-based ceramics [92,145–147]. Our research has led us to the idea that material systems exhibiting R-T phase boundaries are excellent potential candidates for potassium sodium niobate piezoceramics.

3.4. KNN system engineering

It is well-established that KNN's piezoelectric capabilities can be considerably enhanced by establishing phase boundaries using various additives, that is, the development of phase boundaries driven by additives plays a significant role in their enhanced piezoelectric properties. KNN-based materials may have their electrical characteristics altered by other influences. Here, we will provide a high-level overview of the KNN-based piezoceramic engineering.

Many studies are currently investigating how dopants change the $T_{\text{R-O}}$, $T_{\text{O-T}}$ and T_{C} of KNN-based piezoceramics. The effects of several dopants have been studied in depth. Research has looked into a variety of ion dopants, including Li^+ , Sb^{5+} , Ta^{5+} , Zr^{4+} , Hf^{4+} and Ag^+ . The formation of an MPB requires the inclusion of these ions [73,83,84,168]. Increasing the amounts of Sb, Ta, Zr and Hf reduces the $T_{\text{O-T}}$ and lowers the $T_{\text{R-O}}$. The operating range of a piezo material is reduced, and the T_{C} is lowered by Ta, Sb and Hf. With its ability to boost T_{C} while lowering $T_{\text{O-T}}$, Li is a popular dopant for achieving and maintaining a high Curie temperature. Similar to Yang et al. (2020), who employed Ag^+ to obtain high Curie temperature, the $T_{\text{C}} = 250$ °C for a doped KNN based piezo material with high piezoelectric characteristics was attained [169]. Wong et al. (2016) created a high-performance KNN-based piezo material with $T_{\text{C}} = 483$ °C and $d_{33} > 200$ pC/N using Li as a dopant [170]. The increased piezoelectric activity of KNN may potentially be attributable to the presence of other variables. For instance, KNN's A and B sites share valence with Li, Ta and Sb. Therefore, using them can prevent the formation of certain flaws. Safari et al. [171] claimed that the greater electronegativities of Ta^{5+} and Sb^{5+} can raise the covalence of the bonds with respect to Nb^{5+} , leading to increased d_{33} values in (Li, Ta, Sb) co-doped

KNN ceramics. The improved piezoelectric characteristics of KNN-based ceramics were also attributed to the high electronegativity of Sb^{5+} , according to a theory proposed by Gao et al. [129]. Consequently, a number of parameters (electron configuration, ligand field theory, covalence, etc.) are taken into account while attempting to enhance the electrical properties by doping chemicals. Therefore, the introduction of one or more components into KNN might affect distinct phase boundaries; the fundamental benefit of these elements is that they cause a simultaneous change in T_{R-O} , T_{O-T} , and T_C .

In order to solve the densification issue that is present in KNN-based piezoceramics, enhance the sintering temperature, and make the material more temperature stable, oxides are utilised in addition to dopants that are of the ion or perovskite type. The inclusion of ZnO has the potential to improve the thermal stability of KNN [148]. MnO_2 is yet another oxide that sees widespread application in KNN-based piezoceramics. Deng et al. [131] conducted research on the effect of adding MnO_2 to KNLNT. They discovered that adding MnO_2 to the material raised the density, lowered the temperature at which it sintered and, most crucially, improved its piezoelectric capabilities. They were able to produce $d_{33} = 251$ pC/N with doped KNLNT containing 0.1 mol% MnO_2 , which is a greater value than undoped KNLNT. Condurache et al. conducted research in 2019 [172] on the additional step of MnO_2 and showed that the phase structure can be altered by adding MnO_2 either before or after the calcination process. If MnO_2 is supplied before calcination, the ratio of orthorhombic to tetragonal phase is 1.9. Conversely, if MnO_2 is added after calcination, the ratio is 0.7. In 2019, Chen et al. [173] used FeO and MgO oxide types in addition to BaZrO_3 dopant and achieved a piezo material that has a large piezoelectric coefficient and coupling factor, where $d_{33} = 324$ pC/N and $K_P = 59\%$ respectively. This was accomplished by creating a piezo material that was doped with BaZrO_3 . It also has a high Curie temperature, which comes in at 304°C . In order to achieve a good piezoelectric response for KNN-based materials, Zhao et al. [174] utilised Fe_2O_3 and CuO. The results of their investigation demonstrate that CuO-doped KNN has a better electro-strain response than Fe_2O_3 doped KNN does.

Meanwhile, recent research has found that rare earth (RE) elements have unusually large outer electron shells and permit numerous orbital bonding paths with other ions. As a result, local structural heterogeneity is created by rare earth dopants and the interfacial energy barriers between phases/polarization states are lowered [175–177]. It has been reported that rare-earth elements can stabilise and reduce the dissipation factor in dielectric ceramics, both of which are considered to be desirable properties. In a study that showed the existence of a ferroelectric-relaxor transition (T_{f-r}), it was discovered that adding moderate rare earth ions lowered the T_{f-r} . Changing from a relaxor to a ferroelectric due to an applied electric field. T_{f-r} decreased and approached room temperature with the coexistence of nonergodic and ergodic relaxor states, which was responsible for the improved strain property [163,164]. The piezoelectric constant, d_{33} , of BNKT ceramics was raised after optimal Sm^{3+} was added increasing x from 0 to 0.015 increases the value from 150 to 190 pC/N and held steady at 165–180 pC/N between 0.015 and 0.030. One of the promising dopants is yttrium (Y^{3+}), a kind of rare-earth element. This is due to the fact that it improves fatigue endurance, remanent polarisation and leakage current. According to Akmal's findings, the addition of yttrium reduced the electrical resistivity to $2.153 \times 10^6 \Omega$, but at dopant concentrations greater than 0.5 mol%, the resistivity began to increase [178,179]. The addition of Y dopant increases the resistance magnitude in doped KNN films. Since the A-site of has an inherent positive charge, charge imbalance in a doped KNN lattice is compensated by cation vacancies [21,22,180]. Therefore, an increase in Y concentration results in an increase in the number of conduction electrons, leading to a dramatic drop in resistivity. It is often attributed to electrical compensation of the integrated cation [181,182]. Few investigations have found

as Table 2 that improving the piezoelectric characteristics of rare-earth dopants by adding other rare-earth elements is achievable.

Table 2. Rare earth elements as dopants engineering.

Rare earth dopants	d_{33}	Ref.
CeO ₂	132	[182]
Yb ₂ O ₃	390	[183]
Nd ₂ O ₃	250	[184]
Y ₂ O ₃	-	[185]

4. Conclusion

The applications for piezoceramics are extensive. Generators, sensors, actuators, and transducers employ them for a wide variety of tasks, including energy harvesting, strain sensing, active vibration reduction, ultrasonic sonar, distance metre, and so on. When it comes to piezoceramics, PZT is a popular choice. Lead-free alternatives are needed to PZT based piezoceramics because of its high toxicity. This transition from PZT to lead-free piezoceramics is being ensured by the legislation of several countries.

KNN is a potential lead-free material for piezoelectric ceramics, but its poor characteristics and temperature dependence have slowed its development for nearly 50 years since its discovery in the 1950s [183]. Recent research has shown that phase boundary engineering (PBE) can improve KNN systems' electrical properties, making them more appropriate for industrial applications. To compensate for these weaknesses, lead-free piezoceramics like KNN can be doped to improve their characteristics. PBE improves material characteristics by changing phase boundaries. PBE enhances KNN's piezoelectric characteristics through synergistic contributions [184]. Phase engineering has been widely used to increase piezoelectricity in KNN-based ceramics by comparing the effects of standard additives on phase structure [185]. Previous section has discussed the results indicate that PBE has the potential to be a useful technique for enhancing the electrical properties of KNN systems, making them more applicable to industrial settings. Therefore, KNN-based piezoceramics can be improved to replace the role of lead-based ones. In addition to its other desirable properties, piezoceramics based on KNN have a high Curie temperature. However, KNN based piezoceramics have a number of limitations, including a high sintering temperature and a poor piezoelectric coefficient. Sintering aids such as ZnO, MnO₂ and CuO have been studied. By this means, piezoceramic densification during sintering is enhanced. Reducing T_{O-T} and raising T_{O-R} to establish MPB is the key strategy for enhancing the piezoelectric coefficient for KNN based piezoceramics. At the same time, it is important to keep T_C levels high. Other dopants are either T_C decreasing or inactive. However, Li and Ag addition can be utilised to boost T_C . The piezoelectric coefficient and Curie temperature of KNN-based piezoceramics have been reported to be rather high, for example $d_{33} = 451$ pC/N and $T_C = 258$ °C [15], $d_{33} = 440$ pC/N and $T_C = 250$ °C [16] and $d_{33} = 308$ pC/N and $T_C = 328$ °C [25]. The piezoelectric ceramic substance KNN has recently attracted interest as a possible replacement for lead-based piezoceramics in a variety of electrical applications due to their high Curie temperature and piezoelectric coefficient. For instance, KNN has found widespread application as a dielectric material

in various electronic applications. As a result of its high dielectric constant and low dielectric loss, it can be used in capacitors and other energy storage devices. By virtue of its dielectric properties, KNN can improve the functionality and efficiency of electrical equipment. However, KNN's appealing ferroelectric characteristics also find use in sensor and actuator applications [186]. Its piezoelectric properties enable it to convert mechanical energy into electrical signals and vice versa. This makes KNN appropriate for biomedical, automotive and industrial sensors, actuators and transducers. While the phase space and associated properties of KNN in ceramic form have been the subject of extensive research, a similarly robust body of literature for thin film KNN is still in its infancy. Micro-electro-mechanical systems (MEMS) have shown to be an excellent method for developing miniaturised systems and devices that combine mechanical and electrical functions. This innovation has prompted the development of KNN based on thin films. These thin films have high transparency and low absorption in the visible and near-infrared spectrums, in addition to exhibiting ferroelectric behaviour. Moreover, research has switched towards developing methods for producing high-quality films and, more recently, towards applying the material in micro- and nano-electronic devices and biomedical settings. KNN films with enhanced characteristics have been deposited and these have potential applications in micro- and nano electronic devices, as demonstrated by a number of studies that have revealed the film synthesis methodologies, highlighting key results and the challenges connected with synthesis approach [187,188]. As interest in developing lead-free piezoceramics grows, so too does the need for more study into KNN-based piezoceramics. One area where more work needs to be done is in the production of KNN-based piezoceramics. KNN based piezoceramics have been shown to have excellent piezoelectric capabilities and a high curie temperature; further investigation into their mechanical properties, electrical properties and mechanical and electrical fatigue behaviours is recommended. Improvements in these fields of study would aid in making informed choices about the range of possible KNN-based piezoceramics and their respective applications.

Use of AI tools declaration

The authors declare they have not used Artificial Intelligence (AI) tools in the creation of this article.

Acknowledgements

Authors are grateful to the Ministry of Higher Education, Malaysia and Universiti Teknikal Malaysia Melaka (UTeM) under the Fundamental Research Grant Scheme (FRGS), grant No.: FRGS/1/2021/TK0/UTEM/01/2.

Conflict of interest

The authors declare no conflict of interest.

References

1. Ringgaard E, Wurlitzer T, Wolny WW (2011) Properties of lead-free piezoceramics based on alkali niobates. *Ferroelectrics* 319: 97–107. <http://doi.org/10.1080/00150190590965497>
2. Cross E (2004) Lead-free at last. *Nature* 432: 24–25. <https://doi.org/10.1038/nature03142>
3. Jaffe B, Cook WR, Jaffe H (1971) *Piezoelectric Ceramics, Non-Metallic Solids*, London: Academic Press. [https://doi.org/10.1016/0022-460X\(72\)90684-0](https://doi.org/10.1016/0022-460X(72)90684-0)
4. Kumar P, Pattanaik M, Sonia (2013) Synthesis and characterizations of KNN ferroelectric ceramics near 50/50 MPB. *Ceram Int* 39: 65–69. <http://doi.org/10.1016/j.ceramint.2012.05.093>
5. Takenaka T, Nagata H (2005) Current status and prospects of lead-free piezoelectric ceramics. *J Eur Ceram Soc* 25: 2693–2700. <http://doi.org/10.1016/j.jeurceramsoc.2005.03.125>
6. ShROUT TR, Zhang SJ (2007) Lead-free piezoelectric ceramics: Alternatives for PZT? *J Electroceramics* 19: 111–124. <http://doi.org/10.1007/s10832-007-9047-0>
7. Rödel J, Jo W, Seifert KTP, et al. (2009) Perspective on the development of lead-free piezoceramics. *J Am Ceram Soc* 92: 1153–1177. <http://doi.org/10.1111/j.1551-2916.2009.03061.x>
8. Chen K, Zhang F, Li D, et al. (2016) Acceptor doping effects in (K_{0.5}Na_{0.5})NbO₃ lead-free piezoelectric ceramics. *Ceram Int* 42: 2899–2903. <http://doi.org/10.1016/j.ceramint.2015.11.016>
9. Jo W, Dittmer R, Acosta M, et al. (2012) Giant electric-field-induced strains in lead-free ceramics for actuator applications—Status and perspective. *J Electroceram* 29: 71–93. <http://doi.org/10.1007/s10832-012-9742-3>
10. Saito Y, Takao H, Tani T, et al. (2004) Lead-free piezoceramics. *Nature* 432: 84–87. <http://doi.org/10.1038/nature03028>
11. Kim JS, Ahn CW, Lee SY, et al. (2011) Effects of LiNbO₃ substitution on lead-free (K_{0.5}Na_{0.5})NbO₃ ceramics: Enhanced ferroelectric and electrical properties. *Curr Appl Phys* 11: S149–S153. <http://doi.org/10.1016/j.cap.2011.03.049>
12. Liang W, Wu W, Xiao D, et al. (2011) Effect of the addition of CaZrO₃ and LiNbO₃ on the phase transitions and piezoelectric properties of K_{0.5}Na_{0.5}NbO₃ lead-free ceramics. *J Am Ceram Soc* 94: 4317–4322. <http://doi.org/10.1111/j.1551-2916.2011.04660.x>
13. Wu J, Xiao D, Zhu J (2015) Potassium-sodium niobate lead-free piezoelectric materials: Past, present, and future of phase boundaries. *Chem Rev* 115: 2559–2595. <http://doi.org/10.1021/cr5006809>
14. Akmal MMT, Warikh ARM, Azlan UA (2015) Physical and electrical properties enhancement of rare-earth doped-potassium sodium niobate (KNN): A review. *Ceram-Silikatty* 59: 158–163.
15. Zuo R, Rödel J, Chen R, et al. (2006) Sintering and electrical properties of lead-free Na_{0.5}K_{0.5}NbO₃ piezoelectric ceramics. *J Am Ceram Soc* 89: 2010–2015. <http://doi.org/10.1111/j.1551-2916.2006.00991.x>
16. Zuo R, Lv D, Fu J, et al. (2009) Phase transition and electrical properties of lead free (Na_{0.5}K_{0.5})NbO₃-BiAlO₃ ceramics. *J Alloys Compd* 476: 836–839. <http://doi.org/10.1016/j.jallcom.2008.09.123>
17. Benabdallah F, Simon A, Khemakhem H, et al. (2011) Linking large piezoelectric coefficients to highly flexible polarization of lead free BaTiO₃-CaTiO₃-BaZrO₃ ceramics. *J Appl Phys* 109: 124116. <http://doi.org/10.1063/1.3599854>
18. Paul J, Nishimatsu T, Kawazoe Y, et al. (2007) Ferroelectric phase transitions in ultrathin films of BaTiO₃. *Phys Rev Lett* 99: 077601. <https://doi.org/10.1103/PhysRevLett.99.077601>

19. Herber RP, Schneider GA, Wagner S, et al. (2007) Characterization of ferroelectric domains in morphotropic potassium sodium niobate with scanning probe microscopy. *Appl Phys Lett* 90: 2522905. <http://doi.org/10.1063/1.2750395>
20. Wurfel P, Batra IP, Jacobs JT (1973) Polarization instability in thin ferroelectric films. *Phys Rev Lett* 30: 1218–1221. <http://doi.org/10.1103/PhysRevLett.30.1218>
21. Song HC, Kim HC, Kang CY, et al. (2009) Multilayer piezoelectric energy scavenger for large current generation. *J Electroceramics* 23: 301–304. <https://doi.org/10.1007/s10832-008-9439-9>
22. Abazari M, Akdoğan EK, Safari A (2008) Effect of manganese doping on remnant polarization and leakage current in (K_{0.44}, Na_{0.52}, Li_{0.04})(Nb_{0.84}, Ta_{0.10}, Sb_{0.06})O₃ epitaxial thin films on SrTiO₃. *Appl Phys Lett* 92: 212903. <http://doi.org/10.1063/1.2937000>
23. Yoo J, Lee K, Chung K, et al. (2006) Piezoelectric and dielectric properties of (LiNaK)(NbTaSb)O₃ ceramics with variation in poling temperature. *Jpn J Appl Phys* 45: 7444–7448. <https://dx.doi.org/10.1143/JJAP.45.7444>
24. Wang D, Cao M, Zhang S (2012) Investigation of ternary system PbHfO₃-PbTiO₃-Pb (Mg_{1/3}Nb_{2/3})O₃ with morphotropic phase boundary compositions. *J Am Ceram Soc* 95: 3220–3228. <https://doi.org/10.1111/j.1551-2916.2012.05300.x>
25. Ahn CW, Jeong ED, Lee SY, et al. (2010) Enhanced ferroelectric properties of LiNbO₃ substituted Na_{0.5}K_{0.5}NbO₃ lead-free thin films grown by chemical solution deposition. *Appl Phys Lett* 93: 212905. <http://doi.org/10.1063/1.3037214>
26. Hagh NM, Jadidian B, Ashbahian E, et al. (2008) Lead-free piezoelectric ceramic transducer in the donor-doped K_{1/2}Na_{1/2}NbO₃ solid solution system. *IEEE T Ultrason Ferr* 55: 214–224. <http://doi.org/10.1109/TUFFC.2008.630>
27. Courths R, Steiner P, Höchst H, et al. (1980) Photoelectron-spectroscopy investigation and electronic properties of LiNbO₃ crystal surfaces. *Appl Phys* 21: 345–352. <https://doi.org/10.1007/BF00895926>
28. Lin D, Xiao D, Zhu J, et al. (2006) Piezoelectric and ferroelectric properties of lead-free [Bi_{1-y}(Na_{1-xy}Li_x)]_{0.5}Ba_yTiO₃ ceramics. *J Eur Ceram Soc* 26: 3247–3251. <https://doi.org/10.1016/j.jeurceramsoc.2005.09.038>
29. Reaney IM, Damjanovic D (1996) Crystal structure and domain-wall contributions to the piezoelectric properties of strontium bismuth titanate ceramics. *J Appl Phys* 80: 4223–4225. <https://doi.org/10.1063/1.363301>
30. Wu J, Tao H, Yuan Y, et al. (2015) Role of antimony in the phase structure and electrical properties of potassium-sodium niobate lead-free ceramics. *RSC Adv* 5: 14575–14583. <https://doi.org/10.1039/C4RA14271C>
31. Bernard J, Benčan A, Rojac T, et al. (2008) Low-temperature sintering of K_{0.5}Na_{0.5}NbO₃ ceramics. *J Am Ceram Soc* 91: 2409–2411. <https://doi.org/10.1111/j.1551-2916.2008.02447.x>
32. Rubio-Marcos F, Romero JJ, Martín-Gonzalez MS, et al. (2010) Effect of stoichiometry and milling processes in the synthesis and the piezoelectric properties of modified KNN nanoparticles by solid state reaction. *J Eur Ceram Soc* 30: 2763–2771. <https://doi.org/10.1016/j.jeurceramsoc.2010.05.027>
33. López-Juárez R, Novelo-Peralta O, González-García F, et al. (2011) Ferroelectric domain structure of lead-free potassium-sodium niobate ceramics. *J Eur Ceram Soc* 31: 1861–1864. <https://doi.org/10.1016/j.jeurceramsoc.2011.02.031>

34. Shen ZY, Li JF, Wang K, et al. (2010) Electrical and mechanical properties of fine-grained Li/Ta-modified (Na,K)NbO₃-based piezoceramics prepared by spark plasma sintering. *J Am Ceram Soc* 93: 1378–1383. <https://doi.org/10.1111/j.1551-2916.2009.03542.x>
35. Uršič H, Benčan A, Škarabot M, et al. (2010) Dielectric, ferroelectric, piezoelectric, and electrostrictive properties of K_{0.5}Na_{0.5}NbO₃ single crystals. *J Appl Phys* 107: 033705. <https://doi.org/10.1063/1.3291119>
36. Bobnar V, Bernard J, Kosec M. (2004) Relaxorlike dielectric properties and history-dependent effects in the lead-free K_{0.5}Na_{0.5}NbO₃-SrTiO₃ ceramic system. *Appl Phys Lett* 85: 994–996. <http://doi.org/10.1063/1.1779947>
37. Wolny WW (2004) European approach to development of new environmentally sustainable electroceramics. *Ceram Int* 30: 1079–1083. <https://doi.org/10.1016/j.ceramint.2003.12.025>
38. Uesu Y, Matsuda M, Yamada Y, et al. (2002) Symmetry of high-piezoelectric Pb-based complex perovskites at the morphotropic phase boundary: I. Neutron diffraction study on Pb(Zn_{1/3}Nb_{2/3})O₃-9%PbTiO₃. *J Phys Soc Jpn* 71: 960–965. <https://doi.org/10.1143/JPSJ.71.960>
39. Zuo R, Xu Z, Li L (2008) Dielectric and piezoelectric properties of Fe₂O₃-doped (Na_{0.5}K_{0.5})_{0.96}Li_{0.04}Nb_{0.86}Ta_{0.1}Sb_{0.04}O₃ lead-free ceramics. *J Phys Chem Solids* 69: 1728–1732. <http://doi.org/10.1016/j.jpcs.2008.01.003>
40. Park SE, Shrout TR (1997) Ultrahigh strain and piezoelectric behavior in relaxor based ferroelectric single crystals. *J Appl Phys* 82: 1804–1811. <http://doi.org/10.1063/1.365983>
41. Damjanovic D (1998) Ferroelectric, dielectric and piezoelectric properties of ferroelectric thin films and ceramics. *Rep Prog Phys* 61: 1267–1324. <http://doi.org/10.1088/0034-4885/61/9/002>
42. Kittel C (1946) Theory of the structure of ferromagnetic domains in films and small particles. *Phys Rev* 70: 965–971. <http://doi.org/10.1103/PhysRev.70.965>
43. Egerton L, Dillon DM (1959) Piezoelectric and dielectric properties of ceramics in the system potassium-sodium niobate. *J Am Ceram Soc* 42: 438–442. <http://doi.org/10.1111/j.1151-2916.1959.tb12971.x>
44. Noheda B, Cox DE, Shirane G, et al. (1999) A monoclinic ferroelectric phase in the Pb(Zr_{1-x}Ti_x)O₃ solid solution. *Appl Phys Lett* 74: 2059–2061. <http://doi.org/10.1063/1.123756>
45. Guo R, Cross LE, Park SE, et al. (2000) Origin of the high piezoelectric response in PbZr_{1-x}Ti_xO₃. *Phys Rev Lett* 84: 5423–5426. <http://doi.org/10.1103/PhysRevLett.84.5423>
46. Kreisel J, Glazer AM, Jones G, et al. (2000) An X-ray diffraction and Raman spectroscopy investigation of A-site substituted perovskite compounds: The (Na_{1-x}K_x)_{0.5}Bi_{0.5}TiO₃ (0 ≤ x ≤ 1) solid solution. *J Phys Condens Matter* 12: 3267–3280. <http://doi.org/10.1088/0953-8984/12/14/305>
47. Singh AK, Pandey D (2003) Evidence for M_B and M_C phases in the morphotropic phase boundary region of (1-x)[Pb(Mg_{1/3}Nb_{2/3})O₃]-xPbTiO₃: A rietveld study. *Phys Rev B* 67: 064102. <http://doi.org/10.1103/PhysRevB.67.064102>
48. Wang P, Li Y, Lu Y (2011) Enhanced piezoelectric properties of (Ba_{0.85}Ca_{0.15})(Ti_{0.9}Zr_{0.1})O₃ lead-free ceramics by optimizing calcination and sintering temperature. *J Eur Ceram Soc* 31: 2005–2012. <http://doi.org/10.1016/j.jeurceramsoc.2011.04.023>
49. Bilc DI, Orlando R, Shaltaf R, et al. (2008) Hybrid exchange-correlation functional for accurate prediction of the electronic and structural properties of ferroelectric oxides. *Phys Rev B* 77: 165107. <http://doi.org/10.1103/PhysRevB.77.165107>

50. Karaki T, Yan K, Miyamoto T, et al. (2007) Lead-free piezoelectric ceramics with large dielectric and piezoelectric constants manufactured from BaTiO₃ nano-powder. *Jpn J Appl Phys* 46: L97. <http://doi.org/10.1143/JJAP.46.L97>
51. Kakimoto KI, Akao K, Guo Y, et al. (2005) Raman scattering study of piezoelectric (N_{0.5}K_{0.5})NbO₃-LiNbO₃ ceramics. *Jpn J Appl Phys* 44: 7064–7067. <http://doi.org/10.1143/JJAP.44.7064>
52. Keeble DS, Benabdallah F, Thomas PA, et al. (2013) Revised structural phase diagram of (Ba_{0.7}Ca_{0.3}TiO₃)(BaZr_{0.2}Ti_{0.8}O₃). *Appl Phys Lett* 102: 092903. <http://doi.org/10.1063/1.4793400>
53. Zhen Y, Li JF (2006) Normal sintering of (K,Na)NbO₃-based ceramics: Influence of sintering temperature on densification, microstructure, and electrical properties. *J Am Ceram Soc* 89: 3669–3675. <http://doi.org/10.1111/j.1551-2916.2006.01313.x>
54. Buhret CF (1962) Some properties of bismuth perovskites. *J Chem Phys* 36: 798–803. <http://doi.org/10.1063/1.1732613>
55. Schönau KA, Schmitt LA, Knapp M, et al. (2007) Nanodomain structure of Pb[Zr_{1-x}Ti_x]O₃ at its morphotropic phase boundary: Investigations from local to average structure. *Phys Rev B* 75: 184117. <http://doi.org/10.1103/PhysRevB.75.184117>
56. Wylie VEB, Damjanovic D, Klein N, et al. (2010) Structural complexity of (Na_{0.5}Bi_{0.5})TiO₃-BaTiO₃ as revealed by Raman spectroscopy. *Phys Rev B* 82: 104112. <http://doi.org/10.1103/PhysRevB.82.104112>
57. Woodward DI, Knudsen J, Reaney IM (2005) Review of crystal and domain structures in the PbZr_xTi_{1-x}O₃ solid solution. *Phys Rev B* 72: 104110. <http://doi.org/10.1103/PhysRevB.72.104110>
58. Ye ZG, Dong M (2000) Morphotropic domain structures and phase transitions in relaxor-based piezo-/ferroelectric (1-x)Pb(Mg_{1/3}Nb_{2/3})O_{3-x}PbTiO₃ single crystals. *J Appl Phys* 87: 2312–2319. <http://doi.org/10.1063/1.372180>
59. Liu SF, Park SE, Shrout TR, et al. (1999) Electric field dependence of piezoelectric properties for rhombohedral 0.955Pb(Zn_{1/3}Nb_{2/3})O₃-0.045PbTiO₃ single crystals. *J Appl Phys* 85: 2810–2814. <http://doi.org/10.1063/1.369599>
60. Anton EM, Jo W, Damjanovic D, et al. (2011) Determination of depolarization temperature of (Bi_{1/2}Na_{1/2})TiO₃-based lead-free piezoceramics. *J Appl Phys* 110: 094108. <http://doi.org/10.1063/1.3660253>
61. Noblanc O, Gaucher P, Calvarin G (1996) Structural and dielectric studies of Pb(Mg_{1/3}Nb_{2/3})O₃-PbTiO₃ ferroelectric solid solutions around the morphotropic boundary. *J Appl Phys* 79: 4291–4297. <http://doi.org/10.1063/1.361865>
62. Xue D, Zhou Y, Bao H, et al. (2011) Elastic, piezoelectric, and dielectric properties of Ba(Zr_{0.2}Ti_{0.8})O₃-50(Ba_{0.7}Ca_{0.3})TiO₃ Pb-free ceramic at the morphotropic phase boundary. *J Appl Phys* 109: 054110. <http://doi.org/10.1063/1.3549173>
63. Wu J, Wang Y, Xiao D, et al. (2007) Effects of Ag content on the phase structure and piezoelectric properties of (K_{0.44-x}Na_{0.52}Li_{0.04}Ag_x)(Nb_{0.91}Ta_{0.05}Sb_{0.04})O₃ lead-free ceramics. *Appl Phys Lett* 91: 132914. <http://doi.org/10.1063/1.2793507>
64. Matsubara M, Yamaguchi T, Kikuta K, et al. (2004) Sinterability and piezoelectric properties of (K,Na)NbO₃ ceramics with novel sintering aid. *Jpn J Appl Phys* 43: 7159–7163. <http://doi.org/10.1143/JJAP.43.7159>

65. Kounga AB, Zhang ST, Jo W, et al. (2008) Morphotropic phase boundary in $(1-x)\text{Bi}_{0.5}\text{Na}_{0.5}\text{TiO}_{3-x}\text{K}_{0.5}\text{Na}_{0.5}\text{NbO}_3$ lead-free piezoceramics. *Appl Phys Lett* 92: 222902. <http://doi.org/10.1063/1.2938064>
66. Wang K, Li JF (2007) Analysis of crystallographic evolution in $(\text{Na},\text{K})\text{NbO}_3$ -based lead-free piezoceramics by X-ray diffraction. *Appl Phys Lett* 91: 262902. <http://doi.org/10.1063/1.2825280>
67. Akdoğan EK, Kerman K, Abazari M, et al. (2008) Origin of high piezoelectric activity in ferroelectric $(\text{K}_{0.44}\text{Na}_{0.52}\text{Li}_{0.04})-(\text{Nb}_{0.84}\text{Ta}_{0.1}\text{Sb}_{0.06})\text{O}_3$ ceramics. *Appl Phys Lett* 92: 112908. <http://doi.org/10.1063/1.2897033>
68. Elkechai O, Manier M, Mercurio JP (1996) $\text{Na}_{0.5}\text{Bi}_{0.5}\text{TiO}_3$ - $\text{K}_{0.5}\text{Bi}_{0.5}\text{TiO}_3$ (NBT-KBT) system: A structural and electrical study. *Phys Stat Sol* 157: 499–506. <http://doi.org/10.1002/pssa.2211570234>
69. Li F, Zhang S, Xu Z, et al. (2010) Composition and phase dependence of the intrinsic and extrinsic piezoelectric activity of domain engineered $(1-x)\text{Pb}(\text{Mg}_{1/3}\text{Nb}_{2/3})\text{O}_3$ - $x\text{PbTiO}_3$ crystals. *J Appl Phys* 108: 034106. <http://doi.org/10.1063/1.3466978>
70. Zuo R, Fu J (2011) Rhombohedral-tetragonal phase coexistence and piezoelectric properties of $(\text{NaK})(\text{NbSb})\text{O}_3$ - LiTaO_3 - BaZrO_3 lead-free ceramics. *J Am Ceram Soc* 94: 1467–1470. <http://doi.org/10.1111/j.1551-2916.2010.04256.x>
71. Fisher JG, Benčan A, Holc J, et al. (2007) Growth of potassium sodium niobate single crystals by solid state crystal growth. *J Cryst Growth* 303: 487–492. <http://doi.org/10.1016/j.jcrysgro.2007.01.011>
72. Jo W, Seifert KTP, Anton E, et al. (2009) Perspective on the development of lead-free piezoceramics. *J Am Ceram Soc* 92: 1153–1177. <http://doi.org/10.1111/j.1551-2916.2009.03061.x>
73. Zhang S, Xia R, Shrout TR (2007) Lead-free piezoelectric ceramics vs. PZT? *J Electroceram* 19: 251–257. <http://doi.org/10.1007/s10832-007-9056-z>
74. Zuo R, Fu J, Lv D, et al. (2010) Antimony tuned rhombohedral-orthorhombic phase transition and enhanced piezoelectric properties in sodium potassium niobate. *J Am Ceram Soc* 93: 2783–2787. <http://doi.org/10.1111/j.1551-2916.2010.03804.x>
75. Wu J, Xiao D, Wang Y, et al. (2008) CaTiO_3 -modified $[(\text{K}_{0.5}\text{Na}_{0.5})_{0.94}\text{Li}_{0.06}](\text{Nb}_{0.94}\text{Sb}_{0.06})\text{O}_3$ lead-free piezoelectric ceramics with improved temperature stability. *Scripta Mater* 59: 750–752. <http://doi.org/10.1016/j.scriptamat.2008.06.011>
76. Wu J, Xiao D, Wang Y, et al. (2008) Improved temperature stability of CaTiO_3 -modified $[(\text{K}_{0.5}\text{Na}_{0.5})_{0.96}\text{Li}_{0.04}](\text{Nb}_{0.91}\text{Sb}_{0.05}\text{Ta}_{0.04})\text{O}_3$ lead-free piezoelectric ceramics. *J Appl Phys* 104: 024102. <http://doi.org/10.1063/1.2956390>
77. Leontsev SO, Eitel RE (2010) Progress in engineering high strain lead-free piezoelectric ceramics. *Sci Technol Adv Mat* 11: 044302. <http://doi.org/10.1088/1468-6996/11/4/044302>
78. Kosec M, Malič B, Benčan A, et al. (2008) KNN-based piezoelectric ceramics, In: Safari A, Akdoğan EK, *Piezoelectric and Acoustic Materials for Transducer Applications*, Boston: Springer. https://doi.org/10.1007/978-0-387-76540-2_5
79. Liu W, Ren X (2009) Large piezoelectric effect in Pb-free ceramics. *Phys Rev Lett* 103: 257602. <http://doi.org/10.1103/PhysRevLett.103.257602>
80. Jo W, Schaab S, Sapper E, et al. (2011) On the phase identity and its thermal evolution of lead free $(\text{Bi}_{1/2}\text{Na}_{1/2})\text{TiO}_3$ -6 mol BaTiO_3 . *J Appl Phys* 110: 074106. <http://doi.org/10.1063/1.3645054>
81. Wang X, Wu J, Xiao D, et al. (2014) Giant piezoelectricity in potassium-sodium niobate lead-free ceramics. *J Am Chem Soc* 136: 2905–2910. <http://doi.org/10.1021/ja500076h>

82. Cheng X, Wu J, Lou X, et al. (2014) Achieving both giant d_{33} and high T_c in potassium-sodium niobate ternary system. *ACS Appl Mater Interfaces* 6: 750–756. <https://doi.org/10.1021/am404793e>
83. Cheng X, Wu J, Wang X, et al. (2013) Mediating the contradiction of d_{33} and T_c in potassium-sodium niobate lead-free piezoceramics. *ACS Appl Mater Interfaces* 5: 10409–10417. <http://doi.org/10.1021/am403448r>
84. Wang X, Wu J, Xiao D, et al. (2014) New potassium-sodium niobate ceramics with a giant d_{33} . *ACS Appl Mater Interfaces* 6: 6177–6180. <http://doi.org/10.1021/am500819v>
85. Cheng X, Wu J, Wang X, et al. (2014) New lead-free piezoelectric ceramics based on $(K_{0.48}Na_{0.52})(Nb_{0.95}Ta_{0.05})O_3$ - $Bi_{0.5}(Na_{0.7}K_{0.2}Li_{0.1})_{0.5}ZrO_3$. *Dalton Trans* 43: 3434–3442. <http://doi.org/10.1039/c3dt52603h>
86. Liang W, Wang Z, Xiao D, et al. (2012) Effect of new phase boundary on the dielectric and piezoelectric properties of $K_{0.5}Na_{0.5}NbO_3$ - $xBaZrO_3$ - $yBi_{0.5}Na_{0.5}TiO_3$ lead-free ceramics. *Integr Ferroelectr* 139: 63–74. <http://doi.org/10.1080/10584587.2012.737221>
87. Zhang B, Wu J, Cheng X, et al. (2013) Lead-free piezoelectrics based on potassium-sodium niobate with giant d_{33} . *ACS Appl Mater Interfaces* 5: 7718–7725. <http://doi.org/10.1021/am402548x>
88. Liang W, Wu W, Xiao D, et al. (2011) Construction of new morphotropic phase boundary in $0.94(K_{0.42x}Na_{0.6}Ba_xNb_{1-x}Zr_x)O_3$ - $0.06LiSbO_3$ lead-free piezoelectric ceramics. *J Mater Sci* 46: 6871–6876. <http://doi.org/10.1007/s10853-011-5650-1>
89. Munz D, Fett T (2000) *Ceramics: Mechanical Properties, Failure Behaviour, Materials Selection*, Heidelberg: Springer Berlin.
90. Han C, Wu J, Pu C, et al. (2012) High piezoelectric coefficient of Pr_2O_3 -doped $Ba_{0.85}Ca_{0.15}Ti_{0.90}Zr_{0.10}O_3$ ceramics. *Ceram Int* 38: 6359–6363. <http://doi.org/10.1016/j.ceramint.2012.05.008>
91. Kalyani AK, Senyshyn A, Ranjan R (2013) Polymorphic phase boundaries and enhanced piezoelectric response in extended composition range in the lead free ferroelectric $BaTi_{1-x}Zr_xO_3$. *J Appl Phys* 114: 014102. <http://doi.org/10.1063/1.4812472>
92. Miclea C, Tanasoiu C, Miclea CF, et al. (2005) Effect of iron and nickel substitution on the piezoelectric properties of PZT type ceramics. *J Eur Ceram Soc* 25: 2397–2400. <http://doi.org/10.1016/j.jeurceramsoc.2005.03.069>
93. Maurya D, Pramanick A, An K, et al. (2012) Enhanced piezoelectricity and nature of electric-field induced structural phase transformation in textured lead-free piezoelectric $Na_{0.5}Bi_{0.5}TiO_3$ - $BaTiO_3$ ceramics. *Appl Phys Lett* 100: 172906. <http://doi.org/10.1063/1.4709404>
94. Singh AK, Mishra SK, Ragini, et al. (2008) Origin of high piezoelectric response of $Pb(Zr_xTi_{1-x})O_3$ at the morphotropic phase boundary: Role of elastic instability. *Appl Phys Lett* 92: 022910. <http://doi.org/10.1063/1.2836269>
95. Jo W, Daniels JE, Jones JL, et al. (2011) Evolving morphotropic phase boundary in lead-free $(Bi_{1/2}Na_{1/2})TiO_3$ - $BaTiO_3$ piezoceramics. *J Appl Phys* 109: 014110. <http://doi.org/10.1063/1.3530737>
96. Zheng T, Wu J, Cheng X, et al. (2014) High strain in $(K_{0.40}Na_{0.60})(Nb_{0.955}Sb_{0.045})O_3$ - $Bi_{0.50}Na_{0.50}ZrO_3$ lead-free ceramics with large piezoelectricity. *J Mater Chem C* 2: 8796–8803. <http://doi.org/10.1039/c4tc01533a>

97. Zhu X, Xu J, Meng Z (1997) Dielectric and piezoelectric properties of $\text{Pb}(\text{Ni}_{1/3}\text{Nb}_{2/3})\text{O}_3\text{-PbTiO}_3\text{-PbZrO}_3$ ceramics modified with bismuth and zinc substitutions. *J Mater Sci* 32: 4275–4282. <http://doi.org/10.1023/A:1018655419424>
98. Gan BK, Yao K, He X (2007) Complex oxide ferroelectric ceramics $\text{Pb}(\text{Ni}_{1/3}\text{Nb}_{2/3})\text{O}_3\text{-Pb}(\text{Zn}_{1/3}\text{Nb}_{2/3})\text{O}_3\text{-Pb}(\text{Mg}_{1/3}\text{Nb}_{2/3})\text{O}_3\text{-PbZrO}_3\text{-PbTiO}_3$ with a low sintering temperature. *J Am Ceram Soc* 90: 1186–1192. <http://doi.org/10.1111/j.1551-2916.2007.01617.x>
99. Liu Y, Li Q, Qiao L, et al. (2022) Achieving giant piezoelectricity and high property uniformity simultaneously in a relaxor ferroelectric crystal through rare-earth element doping. *Adv Sci* 9: 2204631. <http://doi.org/10.1002/advs.202204631>
100. Tellier J, Malic B, Dkhil B, et al. (2009) Crystal structure and phase transitions of sodium potassium niobate perovskites. *Solid State Sci* 11: 320–324. <https://doi.org/10.1016/j.solidstatesciences.2008.07.011>
101. Baker DW, Thomas PA, Zhang N, et al. (2009) Structural study of $\text{K}_x\text{Na}_{1-x}\text{NbO}_3$ (KNN) for compositions in the range $x = 0.24\text{--}0.36$. *Acta Cryst B* 65: 22–28. <http://doi.org/10.1107/S0108768108037361>
102. Sharma JP, Kumar D, Sharma AK (2021) Structural and dielectric properties of pure potassium sodium niobate (KNN) lead free ceramics. *Solid State Commun* 334–335. <http://doi.org/10.1016/j.ssc.2021.114345>
103. Zheng T, Wu J, Xiao D, et al. (2015) Potassium-sodium niobate lead-free ceramics: Modified strain as well as piezoelectricity. *J Mater Chem A* 3: 1868–1874. <http://doi.org/10.1039/c4ta05423g>
104. Lv X, Wu J, Xiao D, et al. (2018) Structural evolution of the R-T phase boundary in KNN-based ceramics. *J Am Ceram Soc* 101: 1191–1200. <http://doi.org/10.1111/jace.15266>
105. Wang R, Bando H, Katsumata T, et al. (2009) Tuning the orthorhombic-rhombohedral phase transition temperature in sodium potassium niobate by incorporating barium zirconate. *Phys Status Solidi-R* 3: 142–144. <http://doi.org/10.1002/pssr.200903090>
106. Li JF, Wang K, Zhu FY, et al. (2013) (K,Na)NbO₃-based lead-free piezoceramics: Fundamental aspects, processing technologies, and remaining challenges. *J Am Ceram Soc* 96: 3677–3696. <http://doi.org/10.1111/jace.12715>
107. Tennery VJ, Hang KW (1968) Thermal and X-ray diffraction studies of the NaNbO_3 single bond sign KNbO_3 system. *J Appl Phys* 39: 4749–4753. <http://doi.org/10.1063/1.1655833>
108. Dai YJ, Zhang XW, Chen KP (2009) Morphotropic phase boundary and electrical properties of $\text{K}_{1-x}\text{Na}_x\text{NbO}_3$ lead-free ceramics. *Appl Phys Lett* 94: 042905. <http://doi.org/10.1063/1.3076105>
109. Karaki T, Katayama T, Yoshida K, et al. (2013) Morphotropic phase boundary slope of (K,Na,Li)NbO₃-BaZrO₃ binary system adjusted using third component (Bi,Na)TiO₃ additive. *Jpn J Appl Phys* 52: 09KD11. <http://doi.org/10.7567/jjap.52.09kd11>
110. Chao X, Yang Z, Li Z, et al. (2012) Phase structures, electrical properties and temperature stability of $(1-x)[(\text{K}_{0.458}\text{Na}_{0.542})0.96\text{Li}_{0.04}](\text{Nb}_{0.85}\text{Ta}_{0.15})\text{O}_3\text{-xBiFeO}_3$ ceramics. *J Alloys Compd* 518: 1–5. <http://doi.org/10.1016/j.jallcom.2011.11.104>
111. Zhou JJ, Li JF, Cheng LQ, et al. (2012) Addition of small amounts of BiFeO₃ to (Li,K,Na)(Nb,Ta)O₃ lead-free ceramics: Influence on phase structure, microstructure and piezoelectric properties. *J Eur Ceram Soc* 32: 3575–3582. <http://doi.org/10.1016/j.jeurceramsoc.2012.05.019>

112. Li X, Zhu J, Wang M, et al. (2010) BiScO₃-modified (K_{0.475}Na_{0.475}Li_{0.05})(Nb_{0.95}Sb_{0.05})O₃ lead-free piezoelectric ceramics. *J Alloys Compd* 499: L1–L4. <http://doi.org/10.1016/j.jallcom.2010.01.129>
113. Zhang C, Chen Z, Ji WJ, et al. (2011) Crystal structures and electrical properties of (1–x)K_{0.5}Na_{0.5}NbO₃-xBi_{0.8}La_{0.2}FeO₃ lead-free ceramics. *J Alloys Compd* 509: 2425–2429. <http://doi.org/10.1016/j.jallcom.2010.11.037>
114. Wu W, Xiao D, Wu J, et al. (2011) Polymorphic phase transition-induced electrical behavior of BiCoO₃-modified (K_{0.48}Na_{0.52})NbO₃ lead-free piezoelectric ceramics. *J Alloys Compd* 509: L284–L288. <http://doi.org/10.1016/j.jallcom.2011.05.004>
115. Yang H, Zhou C, Zhou Q, et al. (2013) Lead-free (Li,Na,K)(Nb,Sb)O₃ piezoelectric ceramics: Effect of Bi(Ni_{0.5}Ti_{0.5})O₃ modification and sintering temperature on microstructure and electrical properties. *J Mater Sci* 48: 2997–3002. <http://doi.org/10.1007/s10853-012-7078-7>
116. Liu Y, Chu R, Xu Z, et al. (2011) Effects of BiAlO₃ on structure and electrical properties of K_{0.5}Na_{0.5}NbO₃-LiSbO₃ lead-free piezoceramics. *Mater Sci Eng B* 176: 1463–1466. <http://doi.org/10.1016/j.mseb.2011.09.002>
117. Zuo R, Fang X, Ye C (2007) Phase structures and electrical properties of new lead-free (Na_{0.5}K_{0.5})NbO₃-(Bi_{0.5}Na_{0.5})TiO₃ ceramics. *Appl Phys Lett* 90: 092904. <http://doi.org/10.1063/1.2710768>
118. Du H, Zhou W, Luo F, et al. (2008) High T_m lead-free relaxor ferroelectrics with broad temperature usage range: 0.04BiScO₃-0.96(K_{0.5}Na_{0.5})NbO₃. *J Appl Phys* 104: 044104. <http://doi.org/10.1063/1.2969773>
119. Du H, Zhou W, Luo F, et al. (2008) Polymorphic phase transition dependence of piezoelectric properties in (K_{0.5}Na_{0.5})NbO₃-(Bi_{0.5}K_{0.5})TiO₃ lead-free ceramics. *J Phys D Appl Phys* 41: 115413. <http://doi.org/10.1088/0022-3727/41/11/115413>
120. Jiang XP, Yang Q, Yu ZD, et al. (2010) Microstructure and electrical properties of Li_{0.5}Bi_{0.5}TiO₃-modified (Na_{0.5}K_{0.5})NbO₃ lead-free piezoelectric ceramics. *J Alloys Compd* 493: 276–280. <http://doi.org/10.1016/j.jallcom.2009.12.079>
121. Wang R, Xie RJ, Hanada K, et al. (2008) Enhanced piezoelectricity around the tetragonal/orthorhombic morphotropic phase boundary in (Na,K)NbO₃-ATiO₃ solid solutions. *J Electroceramics* 21: 263–266. <http://doi.org/10.1007/s10832-007-9136-0>
122. Park HY, Cho KH, Paik DS, et al. (2007) Microstructure and piezoelectric properties of lead-free (1–x)(Na_{0.5}K_{0.5})NbO₃-xCaTiO₃ ceramics. *J Appl Phys* 102: 124101. <http://doi.org/10.1063/1.2822334>
123. Kim MR, Song HC, Choi JW, et al. (2009) Synthesis and piezoelectric properties of (1–x)(Na_{0.5}K_{0.5})NbO₃-x(Ba_{0.95}Sr_{0.05})TiO₃ ceramics. *J Electroceramics* 23: 502–505. <http://doi.org/10.1007/s10832-008-9519-x>
124. Chen Z, He X, Yu Y, et al. (2009) Piezoelectric and dielectric properties of (Na_{0.5}K_{0.5})NbO₃-(Bi_{0.5}Na_{0.5})_{0.94}Ba_{0.06}TiO₃ lead-free piezoelectric ceramics. *Jpn J Appl Phys* 48: 030204. <http://doi.org/10.1143/JJAP.48.030204>
125. Zuo R, Lv D, Fu J, et al. (2009) Phase transition and electrical properties of lead free (Na_{0.5}K_{0.5})NbO₃-BiAlO₃ ceramics. *J Alloys Compd* 476: 836–839. <http://doi.org/10.1016/j.jallcom.2008.09.123>
126. Du H, Zhou W, Luo F, et al. (2008) Design and electrical properties' investigation of (K_{0.5}Na_{0.5})NbO₃-BiMeO₃ lead-free piezoelectric ceramics. *J Appl Phys* 104: 034104. <https://doi.org/10.1063/1.2964100>

127. Tao H, Wu J, Zheng T, et al. (2015) New $(1-x)\text{K}_{0.45}\text{Na}_{0.55}\text{Nb}_{0.96}\text{Sb}_{0.04}\text{O}_{3-x}\text{Bi}_{0.5}\text{Na}_{0.5}\text{HfO}_3$ lead-free ceramics: Phase boundary and their electrical properties. *J Appl Phys* 118: 044102. <http://doi.org/10.1063/1.4927281>
128. Gao Y, Zhang J, Qing Y, et al. (2011) Remarkably strong piezoelectricity of lead-free $(\text{K}_{0.45}\text{Na}_{0.55})_{0.98}\text{Li}_{0.02}(\text{Nb}_{0.77}\text{Ta}_{0.18}\text{Sb}_{0.05})\text{O}_3$ ceramic. *J Am Ceram Soc* 94: 2968–2973. <http://doi.org/10.1111/j.1551-2916.2011.04468.x>
129. Xu P, Jiang M, Liu X (2011) Effects of low concentration BiFeO_3 additions on microstructure and piezoelectric properties of $(\text{K}_{0.5}\text{Na}_{0.5})\text{NbO}_3$ ceramics. *Adv Mat Res* 335–336: 968–975. <http://doi.org/10.4028/www.scientific.net/AMR.335-336.968>
130. Deng Y, Wang J, Zhang C, et al. (2020) Structural and electric properties of MnO_2 -doped KNN-LT lead-free piezoelectric ceramics. *Crystals* 10: 1–8. <http://doi.org/10.3390/cryst10080705>
131. Zhang Y, Zhai J, Xue S (2020) Effect of three step sintering on piezoelectric properties of KNN-based lead-free ceramics. *Chem Phys Lett* 758: 137906. <http://doi.org/10.1016/j.cplett.2020.137906>
132. Jiang J, Li H, Zhao C, et al. (2022) Broad-temperature-span and improved piezoelectric/dielectric properties in potassium sodium niobate-based ceramics through diffusion phase transition. *J Alloys Compd* 925: 166708. <http://doi.org/10.1016/j.jallcom.2022.166708>
133. Liu Y, Pan Y, Bai X, et al. (2021) Structure evolution and piezoelectric properties of $\text{K}_{0.40}\text{Na}_{0.60}\text{Nb}_{0.95}\text{Sb}_{0.05}\text{O}_3\text{-Bi}_{0.5}\text{K}_{0.5}\text{HfO}_3\text{-SrZrO}_3$ ternary lead-free ceramics with R-O-T phase boundary. *J Mater Sci Mater Electron* 32: 9032–9043. <http://doi.org/10.1007/s10854-021-05573-7>
134. Jiang M, Liu X, Chen G (2009) Phase structures and electrical properties of new lead-free $\text{Na}_{0.5}\text{K}_{0.5}\text{NbO}_3\text{-LiSbO}_3\text{-BiFeO}_3$ ceramics. *Scripta Mater* 60: 909–912. <http://doi.org/10.1016/j.scriptamat.2009.02.017>
135. Minhong J, Manjiao D, Huaxin L, et al. (2011) Piezoelectric and dielectric properties of $\text{K}_{0.5}\text{Na}_{0.5}\text{NbO}_3\text{-LiSbO}_3\text{-BiScO}_3$ lead-free piezoceramics. *Mater Sci Eng B* 176: 167–170. <http://doi.org/10.1016/j.mseb.2010.10.007>
136. Li F, Tan Z, Xing J, et al. (2017) Investigation of new lead free $(1-x)\text{KNNS-xBKZH}$ piezoceramics with R-O-T phase boundary. *J Mater Sci Mater Electron* 28: 8803–8809. <http://doi.org/10.1007/s10854-017-6607-1>
137. Li F, Gou Q, Xing J, et al. (2017) The piezoelectric and dielectric properties of sodium-potassium niobate ceramics with new multiphase boundary. *J Mater Sci Mater Electron* 28: 18090–18098. <http://doi.org/10.1007/s10854-017-7753-1>
138. Qiao L, Li G, Tao H, et al. (2020) Full characterization for material constants of a promising KNN-based lead-free piezoelectric ceramic. *Ceram Int* 46: 5641–5644. <http://doi.org/10.1016/j.ceramint.2019.11.009>
139. Shi C, Ma J, Wu J, et al. (2020) Coexistence of excellent piezoelectric performance and high curie temperature in KNN-based lead-free piezoelectric ceramics. *J Alloys Compd* 846: 156245. <http://doi.org/10.1016/j.jallcom.2020.156245>
140. Pan D, Guo Y, Zhang K, et al. (2017) Phase structure, microstructure, and piezoelectric properties of potassium-sodium niobate-based lead-free ceramics modified by Ca. *J Alloys Compd* 693: 950–954. <http://doi.org/10.1016/j.jallcom.2016.09.277>
141. Wang C, Fang B, Qu Y, et al. (2020) Preparation of KNN based lead-free piezoelectric ceramics via composition designing and two-step sintering. *J Alloys Compd* 832: 153043. <http://doi.org/10.1016/j.jallcom.2019.153043>

142. Politova ED, Kaleva GM, Mosunov AV, et al. (2020) Dielectric and local piezoelectric properties of lead-free KNN-based perovskite ceramics. *Ferroelectrics* 569: 201–208. <http://doi.org/10.1080/00150193.2020.1822677>
143. Brenda CJ, Armando RM, Villafuerte CME, et al. (2018) Piezoelectric, dielectric and ferroelectric properties of $(1-x)(\text{K}_{0.48}\text{Na}_{0.52})_{0.95}\text{Li}_{0.05}\text{Nb}_{0.95}\text{Sb}_{0.05}\text{O}_3-x\text{Ba}_{0.5}(\text{Bi}_{0.5}\text{Na}_{0.5})_{0.5}\text{ZrO}_3$ lead-free solid solution. *J Electron Mater* 47: 6053–6058. <http://doi.org/10.1007/s11664-018-6488-y>
144. Zhang K, Guo Y, Pan D, et al. (2016) Phase transition and piezoelectric properties of dense $(\text{K}_{0.48}\text{Na}_{0.52})_{0.95}\text{Li}_{0.05}\text{Sb}_x\text{Nb}_{(1-x)}\text{O}_3-0.03\text{Ca}_{0.5}(\text{Bi}_{0.5}\text{Na}_{0.5})_{0.5}\text{ZrO}_3$ lead free ceramics. *J Alloys Compd* 664: 503–509. <http://doi.org/10.1016/j.jallcom.2015.12.256>
145. Wendari TP, Arief S, Mufti N, et al. (2020) Ratio effect of salt fluxes on structure, dielectric and magnetic properties of La, Mn-doped $\text{PbBi}_2\text{Nb}_2\text{O}_9$ aurivillius phase. *Ceram Int* 46: 14822–14827. <http://doi.org/10.1016/j.ceramint.2020.03.007>
146. Difeo M, Rubio-Marcos F, Gibbs F, et al. (2023) Effect of antimony content on transition behavior and electric properties of $(\text{K}_{0.44}\text{Na}_{0.52}\text{Li}_{0.04})(\text{Nb}_{0.9-x}\text{Ta}_{0.10}\text{Sb}_x)\text{O}_3$ ceramics. *Appl Sci* 13: 992. <https://doi.org/10.3390/app13020992>
147. Wu J (2018) *Advances in Lead-Free Piezoelectric Materials*, Singapore: Springer Singapore. <https://doi.org/10.1007/978-981-10-8998-5>
148. Nandini RN, Krishna M, Suresh AV, et al. (2018) Effect of MWCNTs on piezoelectric and ferroelectric properties of KNN composites. *Mater Sci Eng B* 231: 40–56. <http://doi.org/10.1016/j.mseb.2018.09.001>
149. Shirane G, Newnham R, Pepinsky R (1954) Dielectric properties and phase transitions of NaNbO_3 and $(\text{Na,K})\text{NbO}_3$. *Phys Rev* 96: 581–588. <http://doi.org/10.1103/PhysRev.96.581>
150. Jaeger Re, Egerton L (1962) Hot pressing of potassium-sodium niobates. *J Am Ceram Soc* 45: 209–213. <http://doi.org/10.1111/j.1151-2916.1962.tb11127.x>
151. Zhang B, Wu J, Wang X, et al. (2013) Rhombohedral-orthorhombic phase coexistence and electrical properties of Ta and BaZrO_3 co-modified $(\text{K,Na})\text{NbO}_3$ lead-free ceramics. *Curr Appl Phys* 13: 1647–1650. <http://doi.org/10.1016/j.cap.2013.06.010>
152. Lv YG, Wang CL, Zhang JL, et al. (2009) Tantalum influence on physical properties of $(\text{K}_{0.5}\text{Na}_{0.5})(\text{Nb}_{1-x}\text{Ta}_x)\text{O}_3$ ceramics. *Mater Res Bull* 44: 284–287. <http://doi.org/10.1016/j.materresbull.2008.06.019>
153. Zuo R, Ye C, Fang X (2007) Dielectric and piezoelectric properties of lead free $\text{Na}_{0.5}\text{K}_{0.5}\text{NbO}_3-\text{BiScO}_3$ ceramics. *Jpn J Appl Phys* 46: 6733–6736. <http://doi.org/10.1143/jjap.46.6733>
154. Zhou C, Zhang J, Yao W, et al. (2018) Piezoelectric performance, phase transitions and domain structure of $0.96(\text{K}_{0.48}\text{Na}_{0.52})(\text{Nb}_{0.96}\text{Sb}_{0.04})\text{O}-0.04(\text{Bi}_{0.50}\text{Na}_{0.50})\text{ZrO}_3$ ceramics. *J Appl Phys* 124: 164101. <http://doi.org/10.1063/1.5048345>
155. Zhang Y, Li P, Shen B, et al. (2018) Effect of shifting orthorhombic-tetragonal phase transition on structure and properties of $\text{K}_{0.5}\text{Na}_{0.5}\text{NbO}_3$ -based lead-free ceramics. *J Alloys Compd* 735: 1328–1330. <http://doi.org/10.1016/j.jallcom.2017.11.281>
156. Guo Y, Kakimoto KI, Ohsato H (2004) Phase transitional behavior and piezoelectric properties of $(\text{Na}_{0.5}\text{K}_{0.5})\text{NbO}_3-\text{LiNbO}_3$ ceramics. *Appl Phys Lett* 85: 4121–4123. <http://doi.org/10.1063/1.1813636>
157. Guo Y, Kakimoto K, Ohsato H (2005) $(\text{Na}_{0.5}\text{K}_{0.5})\text{NbO}_3-\text{LiTaO}_3$ lead-free piezoelectric ceramics. *Mater Lett* 59: 241–244. <https://doi.org/10.1016/j.matlet.2004.07.057>

158. Wang K, Li JF, Liu N (2008) Piezoelectric properties of low-temperature sintered Li-modified (Na,K)NbO₃ lead-free ceramics. *Appl Phys Lett* 93: 092904. <http://doi.org/10.1063/1.2977551>
159. Wang R, Bando H, Itoh M (2009) Universality in phase diagram of (K,Na)NbO₃-MTiO₃ solid solutions. *Appl Phys Lett* 95: 092905. <http://doi.org/10.1063/1.3224196>
160. Wang R, Bando H, Kidate M, et al. (2011) Effects of A-site ions on the phase transition temperatures and dielectric properties of (1-x)(Na_{0.5}K_{0.5})NbO₃-xAZrO₃ solid solutions. *Jpn J Appl Phys* 50: 09ND10. <http://doi.org/10.1143/JJAP.50.09ND10>
161. Zheng T, Wu J, Cheng X, et al. (2014) Wide phase boundary zone, piezoelectric properties, and stability in 0.97(K_{0.4}Na_{0.6})(Nb_{1-x}Sb_x)O₃-0.03Bi_{0.5}Li_{0.5}ZrO₃ lead-free ceramics. *Dalton Trans* 43: 9419–9426. <http://doi.org/10.1039/c4dt00768a>
162. Fong DD, Kolpak AM, Eastman JA, et al. (2006) Stabilization of monodomain polarization in ultrathin PbTiO₃ films. *Phys Rev Lett* 96: 127601. <http://doi.org/10.1103/PhysRevLett.96.127601>
163. Wang X, Wu J, Xiao D, et al. (2014) Giant piezoelectricity in potassium-sodium niobate lead-free ceramics. *J Am Chem Soc* 136: 2905–2910. <http://doi.org/10.1021/ja500076h>
164. Wang X, Wu J, Cheng X, et al. (2013) Compositional dependence of phase structure and electrical properties in (K_{0.50}Na_{0.50})_{0.97}Bi_{0.01}(Nb_{1-x}Zr_x)O₃ lead-free ceramics. *Ceram Int* 39: 8021–8024. <http://doi.org/10.1016/j.ceramint.2013.03.071>
165. Zheng T, Wu J, Cheng X, et al. (2014) New potassium-sodium niobate material system: A giant-d₃₃ and high-T_C lead-free piezoelectric. *Dalton Trans* 43: 11759–11766. <http://doi.org/10.1039/c4dt01293c>
166. Yang W, Li P, Wu S, et al. (2020) Coexistence of excellent piezoelectric performance and thermal stability in KNN-based lead-free piezoelectric ceramics. *Ceram Int* 46: 1390–1395. <http://doi.org/10.1016/j.ceramint.2019.09.102>
167. Wong JYY, Zhang N, Ye ZG (2016) High-temperature solution growth and vapour transport equilibration of (1-x)K_{1-y}Na_yNbO₃-xLiNbO₃ lead-free piezo-/ferroelectric single crystals. *J Cryst Growth* 452: 125–130. <http://doi.org/10.1016/j.jcrysgro.2016.01.022>
168. Priya S, Nahm S (2013) *Lead-Free Piezoelectrics*, New York: Springer New York. <https://doi.org/10.1007/978-1-4419-9598-8>
169. Condurache OA, Radan K, Prah U, et al. (2019) Heterogeneity challenges in multiple-element-modified lead-free piezoelectric ceramics. *Materials* 12: 4049. <https://doi.org/10.3390/ma12244049>
170. Chen R, Jiang L, Zhang T, et al. (2019) Eco-friendly highly sensitive transducers based on a new KNN-NTK-FM lead-free piezoelectric ceramic for high-frequency biomedical ultrasonic imaging applications. *IEEE Trans Biomed Eng* 66: 1580–1587. <http://doi.org/10.1109/TBME.2018.2876063>
171. Zhao Z, Lv Y, Dai Y, et al. (2020) Ultrahigh electro-strain in acceptor-doped KNN lead-free piezoelectric ceramics via defect engineering. *Acta Mater* 200: 35–41. <http://doi.org/10.1016/j.actamat.2020.08.073>
172. Zhang Y, Li JF (2019) Review of chemical modification on potassium sodium niobate lead-free piezoelectrics. *J Mater Chem C* 7: 4284–4303. <http://doi.org/10.1039/c9tc00476a>
173. Schütz D, Deluca M, Krauss W, et al. (2012) Lone-pair-induced covalency as the cause of temperature and field-induced instabilities in bismuth sodium titanate. *Adv Funct Mater* 22: 2285–2294. <http://doi.org/10.1002/adfm.201102758>

174. Yin J, Zhao C, Zhang Y, et al. (2018) Ultrahigh strain in site engineering-independent $\text{Bi}_{0.5}\text{Na}_{0.5}\text{TiO}_3$ -based relaxor-ferroelectrics. *Acta Mater* 147: 70–77. <http://doi.org/10.1016/j.actamat.2018.01.054>
175. Akmal MHM, Warikh ARM, Azlan UAA, et al. (2016) Structural evolution and dopant occupancy preference of yttrium-doped potassium sodium niobate thin films. *J Electroceramics* 37: 50–57. <http://doi.org/10.1007/s10832-016-0039-9>
176. Akmal MHM, Warikh ARM (2021) Electrical behaviour of yttrium-doped potassium sodium niobate thin film for piezoelectric energy harvester applications. *J Aust Ceram Soc* 57: 589–596. <http://doi.org/10.1007/s41779-021-00569-2>
177. Knauth P (2006) Ionic and electronic conduction in nanostructured solids: Concepts and concerns, consensus and controversies. *Solid State Ionics* 177: 2495–2502. <http://doi.org/10.1016/j.ssi.2006.02.039>
178. Maziaty A, Umar A, Warikh M, et al. (2015) Enhanced structural and electrical properties of lead-free Y-doped $(\text{K},\text{Na})\text{NbO}_3$ thin films. *Jurnal Teknologi* 77: 67–71. <https://doi.org/10.11113/jt.v77.6609>
179. Li Y, Chen W, Xu Q, et al. (2007) Piezoelectric and dielectric properties of CeO_2 -doped $\text{Bi}_{0.5}\text{Na}_{0.44}\text{K}_{0.06}\text{TiO}_3$ lead-free ceramics. *Ceram Int* 33: 95–99. <http://doi.org/10.1016/j.ceramint.2005.08.001>
180. Deng A, Wu J (2020) Effects of rare-earth dopants on phase structure and electrical properties of lead-free bismuth sodium titanate-based ceramics. *J Materiomics* 6: 286–292. <http://doi.org/10.1016/j.jmat.2020.03.005>
181. Bathelt R, Soller T, Benkert K, et al. (2012) Neodymium doping of KNNLT. *J Eur Ceram Soc* 32: 3767–3772. <http://doi.org/10.1016/j.jeurceramsoc.2012.05.025>
182. Akmal M, Hatta M, Warikh ARM, et al. (2016) Influence of yttrium dopant on the structure and electrical conductivity of potassium sodium niobate thin films. *Mat Res* 19: 1417–1422. <https://doi.org/10.1590/1980-5373-MR-2016-0076>
183. Lv X, Zhu J, Xiao D, et al. (2020) Emerging new phase boundary in potassium sodium-niobate based ceramics. *Chem Soc Rev* 49: 671–707. <http://doi.org/10.1039/c9cs00432g>
184. Lv X, Zhang J, Liu Y, et al. (2020) Synergetic contributions in phase boundary engineering to the piezoelectricity of potassium sodium niobate lead-free piezoceramics. *ACS Appl Mater Interfaces* 12: 39455–39461. <http://doi.org/10.1021/acsami.0c12424>
185. Ma ZY, Zheng HJ, Zhao L, et al. (2023) Comparison of impact from typical additives for phase structure in $(\text{K},\text{Na})\text{NbO}_3$ -based ceramics. *Ceram Int* 49: 18629–18637. <http://doi.org/10.1016/j.ceramint.2023.02.239>
186. Dahiya A, Thakur OP, Juneja JK (2013) Sensing and actuating applications of potassium sodium niobate: Use of potassium sodium niobate in sensor and actuator. 2013 Seventh International Conference on Sensing Technology (ICST), New Zealand, 383–386.
187. Maziaty Akmal MH, Warikh ARM, Azlan UAA, et al. (2017) The effects of different annealing temperatures and number of deposition layers on the crystallographic properties sodium niobate (KNN) thin films synthesized by sol-gel spin coating technique. *J Adv Manuf Technol* 11: 91–102. Available from: <https://jamt.utem.edu.my/jamt/article/view/1232>.

-
188. Akmal MHM, Warikh ARM, Azlan UAA, et al. (2018) Optimizing the processing conditions of sodium potassium niobate thin films prepared by sol-gel spin coating technique. *Ceram Int* 44: 317–325. <https://doi.org/10.1016/j.ceramint.2017.09.175>



AIMS Press

© 2023 the Author(s), licensee AIMS Press. This is an open access article distributed under the terms of the Creative Commons Attribution License (<http://creativecommons.org/licenses/by/4.0>)